Available online at www.sciencedirect.com
SCIENCE DIRECT®
Journal of Chromatography A, 1037 (2004) 147–189
JOURNAL OF CHROMATOGRAPHY A
www.elsevier.com/locate/chroma

Review

Determination of diffusion coefficients by gas chromatography

George Karaiskakis*, Dimitrios Gavril

Department of Chemistry, University of Patras, 26504 Patras, Greece

Abstract

Gas chromatography (GC), apart from the qualitative and quantitative analysis of gaseous mixtures, offers many possibilities for physicochemical measurements, among which the most important is the determination of diffusion coefficients of gases in gases and liquids and on solids. The gas chromatographic techniques used for the measurement of diffusion coefficients, namely the methods based on the broadening of the chromatographic elution peaks, and those based on the perturbation of the carrier gas flow-rate, are reviewed from the GC viewpoint, considering their running though the history, the experimental arrangement and procedure, the appropriate mathematical analysis and the main results with brief discussions. The experimental data on diffusion coefficients, determined by the various gas chromatographic techniques, are compared with those quoted in the literature or estimated by the known empirical equations predicting diffusion coefficients. This comparison permits the calculation of the precision and accuracy of the techniques applied to the measurement of diffusion coefficients.

Keywords: Reviews; Diffusion coefficients; Gas chromatography

Contents

* Corresponding author. Tel.: +30-2610-997144;
fax: +30-2610-997144.
E-mail address: g.karaiskakis@chemistry.upatras.gr (G. Karaiskakis).

0021-9673/$ – see front matter © 2004 Elsevier B.V. All rights reserved.
doi:10.1016/j.chroma.2004.01.015

1. Introduction

Knowledge of diffusion coefficients is important in many areas of both basic and engineering research and in chromatography. The binary diffusion coefficients of gases are needed in the design of reactors where gas-phase reactions are involved. Diffusion may plays an important role in chemical reactions and must be considered in the design of distillation columns. It has important applications to global changes, atmospheric chemistry, combustion science, studies of indoor air pollution and atmosphere–biosphere interactions. Diffusion is also a major factor in peak broadening in chromatography. Therefore, accurate and reliable values of diffusion coefficients are necessary in the testing of chromatographic theory.

Moreover, binary diffusion measurements lead to the determination of collision cross-sections. In the past, collision cross-section measurements had been based mainly on viscosity data and molecular beam scattering measurements. Binary diffusion coefficient is a better tool, since it is a direct measure of interaction between dissimilar molecules.

Although coefficients of diffusivity have been experimentally determined by various techniques for over a century, there is still considerable variation in the values quoted by different researchers and references.

The diffusion coefficients can be determined by various gas chromatographic techniques based either on the broadening of the elution peaks, or on the perturbation imposed on the carrier gas flow-rate.

2. Diffusion in gases

2.1. Empirical equations

The mass diffusivity D_{AB} for a binary system is a function of temperature, pressure, and composition. The data available on D_{AB} for most binary mixtures are, moreover, quite limited in range and accuracy. For binary gas mixtures at low pressure, D_{AB} is inversely proportional to the pressure, increases with increasing temperature, and is almost independent of composition for a given gas-pair. For an n-component ideal-gas mixture, the mass diffusivity D_{ij} of the pair i–j is concentration dependent. These variations are all described, with different degrees of precision, by the following empirical equations of the kinetic theory of gases, which are used for the prediction of the D_{AB} values [1].

(i) The Stefan–Maxwell (SM) equation:

$$D_{AB} = \frac{a}{n\sigma_{AB}^2} \cdot \left[\frac{8RT}{\pi} \cdot \left(\frac{1}{M_A} + \frac{1}{M_B}\right)\right]^{1/2} \quad (1)$$

where a is a constant taking various values ($1/3\pi$, 1/8, $1/2\pi$ and 3/32) depending on the proposer researcher, n is the number of gas phase molecules per cm^3, σ_{AB} is the collision diameter between the gas molecules A and B, R is the gas constant, T is the absolute temperature and M_A, M_B are the molecular masses of solute A and carrier gas B, respectively.

(ii) The Chapman–Enskog equation:

$$D_{AB} = \frac{0.00263T^{3/2}}{p\sigma_{AB}^2} \cdot \left(\frac{1/M_A + 1/M_B}{2}\right)^{1/2} \quad (2)$$

where p is the gas pressure in atm.

(iii) The Gilliland equation:

$$D_{AB} = \frac{0.0043T^{3/2}(1/M_A + 1/M_B)^{1/2}}{p(V_A^{1/3} + V_B^{1/3})} \quad (3)$$

where V_A and V_B are molar volumes in cm^3, at the boiling points, which can be obtained directly, or they can be estimated as an additive sum of the volume of molecular constituents.

(iv) The Arnold equation:

$$D_{AB} = \frac{0.0083T^{3/2}(1/M_A + 1/M_B)^{1/2}}{p(V_A^{1/3} + V_B^{1/3})(1 + c_{AB}/T)} \quad (4)$$

where c_{AB} is Sutherland's constant, which can be estimated by various ways. The above equation, which introduces a second temperature dependent term in the denominator to account for molecular "softness", shows a dependence varying from $T^{3/2}$ to $T^{5/2}$.

(v) The Hirschfelder–Bird–Spotz (HBS) equation:

$$D_{AB} = \frac{0.00186T^{3/2}(1/M_A + 1/M_B)^{1/2}}{p\sigma_{AB}^2\Omega_{AB}} \quad (5)$$

The term Ω_{AB} is the collision integral depending in a complicated way on temperature and the interaction energy of the colliding molecules, ε_{AB}. Hirschfelder et al. [2] followed the Chapman–Enskog kinetic approach combined with the Lennard–Jones intermolecular (6–12) potential function. Ω_{AB} values as function of the reduced temperature $T^* = kT/\varepsilon_{AB}$, where k is the Boltzmann constant, have been tabulated [2,3]. The main disadvantage of the HBS equation is the difficulty encountered in evaluating σ_{AB} and Ω_{AB}. Most such values have been obtained from viscosity measurements.

(vi) Chen and Othmer provided the most explicit approximation of the HBS equation using the critical values of temperature, T_C, and volume, V_C:

$$D_{AB} = \frac{0.43(T/100)^{1.81}(1/M_A + 1/M_B)^{1/2}}{p(T_{CA}T_{CB}/10^4)^{0.1405}[(V_{CA}/100)^{0.4} + (V_{CB}/100)^{0.4}]^2} \quad (6)$$

Both T_C and V_C values can be estimated in various ways [1,2].

Table 1
Atomic diffusion contributions for $\sum v$ in Eq. (7)

Diffusion volumes of single molecules							
He	2.67	H_2	6.12	CO	18.0	SF_6	71.3
Ne	5.98	D_2	6.84	CO_2	26.9	Cl_2	38.4
Ar	16.2	N_2	18.5	N_2O	35.9	Br_2	69.0
Kr	24.5	O_2	16.3	NH_3	20.7	SO_2	41.8
Xe	32.7	Air	19.7	H_2O	13.1		
Atomic and structural diffusion volume increments							
C	15.9	N	4.54	F	14.7	I	29.8
H	2.31	Aromatic ring	−18.3	Cl	21.0	S	22.9
O	6.11	Heterocyclic ring	−18.3	Br	21.9		

Table 2
Average percentage accuracy of various methods tested for the prediction of binary gaseous diffusion coefficients for 134 literature D_{AB} values [6]

Method	Accuracy (%)
Gilliland	6.64
Arnold	11.75
Hirschfelder–Bird–Spotz	18.99
Chen–Othmer	10.85
Fuller–Schettler–Giddings	3.40
Huang–Young–Huang–Kuo	3.51

$$\text{Accuracy (\%)} = \left|\frac{D_{AB}^{exp} - D_{AB}^{calcd}}{D_{AB}^{exp}}\right| \times 100 .$$

(vii) Fuller–Schettler and Giddings [4,5] developed a successful equation in which atomic and structural volume increments and other parameters were obtained by a least-squares fit to over 300 measurements. In the Fuller et al. method:

$$D_{AB} = \frac{0.00143T^{1.75}(1/M_A + 1/M_B)^{1/2}}{p\left[(\sum v)_A^{1/3} + (\sum v)_B^{1/3}\right]^2} \quad (7)$$

$\sum v$ is determined by summing the atomic contributions shown in Table 1.

(viii) Huang et al. [6] investigated the effects of pressure and temperature on the gas diffusivity. Based on their experimental data they modificated the Arnold equation as follows:

$$D_{AB} = \frac{5.06T^{1.75}(1/M_A + 1/M_B)^{1/2}}{p^{1.286}(V_A^{1/3} + V_B^{1/3})^2} \quad (8)$$

They compared Eq. (8) with the most of the equations applied to the other techniques. They used for their comparison 134 literature diffusion coefficient values. The results of this comparison are given in Table 2.

For high precision in estimating gaseous diffusion coefficient values, the more complicated methods derived from

the HBS equation should be used. These methods based on detailed gas dynamics, are undoubtedly valid for unusual systems (e.g. large molecules, high temperatures, etc.) for which the Gilliland and Arnold equations are not tested. The Fuller–Schettler–Giddings (FSG) equation provides the best practical combination of simplicity and accuracy.

2.2. The broadening techniques

Marrero and Mason [7] have written an excellent review on gaseous diffusion for all the known methods of obtaining such data, including the gas chromatographic method. This method, first introduced by Giddings [8], has been used by many other workers in its original form and in several other modified forms. Both, Giddings' gas chromatographic method and its modifications, which are based on the broadening of the chromatographic bands, are known as gas chromatographic broadening techniques (GC-BT). An excellent review, for the measurement of gas–gas and gas–liquid vapor binary diffusion coefficients, by methods based on the broadening of the elution peaks, has been written by Maynard and Grushka [9].

2.2.1. Historical review

It is useful to present shortly the methods used for the measurement of gas diffusion coefficients before the gas chromatographic method.

The closed-tube technique was developed by Loschmidt [10,11] in 1870. The apparatus consists of a long tube closed at both ends with a fast opening valve in the middle. In the methodology of closed-tube technique, initially separated samples of the pure gases are allowed to mix by diffusion, and the determination of the composition of each section is done after a period of time. The precision and accuracy of the method are quite good and the apparatus yields excellent values for binary gas systems. Its main disadvantage is the relatively long analysis time.

Ney and Armstead [12] improved the closed-tube method developing the two-bulb apparatus. The two diffusion gases are contained into the bulbs joined by a narrow tube. As a result the device is more compact and easier to thermostat. The precision and accuracy of the two-bulb and close-tube devices are similar.

Stefan [13] developed in 1873, the evaporation-tube method for measuring the diffusion coefficients of liquid vapor–gas mixtures. A liquid or volatile solid is placed in the bottom of a short tube. In this technique the loss of the material through evaporation is measured. The method has poor precision (>5%) and the measurements are time consuming (half a day).

Westenberg and Walker [14] developed the point-source method, which is very similar to the gas chromatographic method, except that the tracer is continuously steaming into the carrier gas. The point-source method has an average accuracy of 5%, and diffusion coefficients have been measured at temperatures of up to 1900 K.

It is generally assumed that the first paper on the use of gas chromatography (GC) to determine diffusion coefficients is that of Giddings and Seager [8]. They used a commercial GC apparatus where the packed column is replaced with a coiled, long and empty tube of circular cross-section. The major importance of that paper is the potential of the described technique as a fast and accurate method of determining gaseous diffusion coefficients. The precision of their measurements (diffusion of hydrogen in carrier gas nitrogen at different flow velocities) was estimated to be about 2% and the accuracy (compared to literature values) was about 5%. The authors also predicted that the technique could be used to calculate diffusion coefficients in liquids.

Bohemen and Purnel [15] published at the next year (1961) a paper describing the measurement of diffusion coefficients at very low velocities using unpacked columns and no correction tube. They showed that the Van Deemter equation reduces to $H = A + B'/\upsilon'$ from which D_{AB} is found by plotting H versus $1/\upsilon'$, as $B' = 2\gamma D_{AB}$ (γ being the destructive factor and υ' the outlet velocity at 1 atm; 1 atm = 101 325 Pa).

Another interesting paper, published independently and almost simultaneously (1961), on diffusion coefficient measurements is that of Fejes and Czaran [16]. They derived diffusion equations useful in frontal analysis. Doing frontal GC studies on equilibria and kinetic relationships concerning adsorption, they needed a better knowledge of diffusion in open and filled tubes. A four-way valve, permitting to switch from a stream of one gas to another, making a step-function injection was included in the experimental setup of a typical gas chromatograph. Their data agreed well with the literature values, but their equations, derived for the case of frontal analysis, are not directly usable for the more generally used elution analysis technique.

In 1962, Giddings and Seager [17] published their second paper on diffusion coefficient measurement. It was more detailed and included more data. The speed of the method was very high, permitting 200 separate determinations in 36 h, while the precision was of about 1%. Such number of measurements would be quite difficult with the older, more time-consuming, methods.

A year later, Knox and McLaren [18] determined the discussion coefficient of nitrogen–ethylene system in order to verify a new equation proposed by them, relating H with υ'.

In the same year, Seager et al. [19] published a paper concerning the temperature dependence of gas–gas and gas–liquid vapor diffusion coefficients. Their method was applied for first time to the measurement of gas–vapor diffusion coefficients. Such measurement can be achieved by using a sensitive detector, to range well above and bellow the boiling point of the mother liquid. The latter was very time consuming when conventional techniques, such as the evaporation-tube method of Stefan [13] were employed. The authors studied the temperature dependence of the diffusion coefficient on various binary gas mixtures containing He as one component and Ar, CO_2, N_2, O_2, benzene, methanol,

ethanol, 1-propanol, 2-pronanol, 1-butanol, 1-pentanol and 1-hexanol as the other component, over a 100–200 °C temperature range. The average for all gases and vapors yields an exponent value equal to 1.70.

Knox and McLaren [20], described in 1964 a new gas chromatographic elution method for measuring gaseous diffusion coefficients and obstructive factors. They called the new method as arrested elution method, and it was an improvement of the continuous elution method. The latter had been much improved by Giddings and Seager [8,17,19] who had employed the full potentialities of the open tube. By using a gas velocity which differs from that required for minimum H (by a factor of at least two) either higher or lower, the diffusion coefficient was then derived by solving the Golay equation (see Section 2.2.2). The difficulties associated with the use of very low flow-rates could thus be avoided. However, an inherent weakness of the continuous elution method was that some broadening factors such as racetrack, secondary flow, concentration effect, end effect, and the buoyant effect of the solute–solvent pair, etc., cannot be isolated in the same run of experiment. For the correction of the above extra zone broadening factors Giddings and Seager [18] introduced the use of the two different length columns (see Section 2.2.3) in two experiments conducted under the same conditions. Unfortunately, identity of two separate sets of experiments is difficult to achieve, especially after the exchange of the column. Therefore, the correction of extra zone broadening factors in the continuous elution method becomes a very difficult task for precision work.

The arrested elution method as used by Knox and McLaren [20] was basically the same as the continuous elution method, except the carrier gas flow was arrested when the solute zone had migrated about half-way along the column. The solute zone was then allowed free molecular diffusion for a time, and finally eluted from the column by resuming the carrier flow. The experiment then was repeated for the same velocity and different arrested times. The total variance measured was then plotted against the arrested time. This yielded a straight line whose slope was $2D_{AB}/\bar{v}^2$ (see Section 2.2.3.2), and therefore by knowing the average carrier velocity, $\bar{v}$, the binary diffusion coefficient, D_{AB}, can be calculated. The experiment was then repeated with packed columns. In that case D_{AB} must be replaced with γD_{AB}, and the obstructive factor, γ, can also be calculated. Using the arrested elution method, the authors determined D_{AB} and γ for the system ethylene in nitrogen.

The major advantage of the arrested elution method is that, band broadening due to flow irregularities is held constant throughout the experiment and is effectively canceled out. Also, the column can be very short and hence decrease the possible error introduced by the pressure drop between the inlet and outlet of a long, especially packed column. Moreover, no assumptions are made about the precise form of the flow profile (which is assumed to be parabolic in the Taylor equation), the smoothness of the column wall, or the accuracy with which the column diameter is known. The authors state that there was little difficulty in arresting the flow so long as the pressure drop across the column was small ($\leq$2 cmHg; 1 cmHg = 1333.22 Pa). It also has to be recognized that the need for several runs, which may involve a period of 2–5 h, to get a D_{AB} value with a precision of about 2%, may degrade the purpose of using GC as a rapid method in determining diffusion coefficient values.

Fuller and Giddings [21] compared the existing theoretical or empirical equations for predicting gaseous diffusion coefficients. Using experimental values for 38 binary gas systems they compared those with the respective values estimated by the different equations, and tabulated the percentage errors for each estimation. The method of Fuller et al. [4] gave the best estimate (see Section 2.1). Average absolute percentage errors varied from 4.2 to 20%, depending on the method employing. In both works [4,21], no new experimental data were given, but their papers show the difficulty in estimating theoretically diffusion coefficients.

Chang [22] determined diffusion coefficients for nitrogen–helium systems using a gas chromatograph of his own design, at pressures ranging from atmospheric to 900 psig and temperatures from 244 to 311 K, as well as for trace amounts of ethane, propane and *n*-butane in methane at 1 atm and in the same temperature range. The found diffusivities compared well with the available literature values and their pressure variation compared well with kinetic theory predictions.

Arnikar et al. [23] illustrated the usefulness of an electrodeless discharge tube as a GC detector, measuring the diffusion coefficient of oxygen in nitrogen in a packed column. They based on the Van Deemter equation to calculate the diffusion coefficient. Their electrodeless discharge detector was used to obtain the peak profile. It appears from 2 to about 14% higher than the respective literature D_{AB} values, that there is no real advantage of using packed columns. Their assumption of $\gamma = 1$ is probably not valid and could account for the large errors.

Giddings and Mallik [24] reviewed “unorthodox” applications of GC, among which the measurement of diffusion coefficients. They reported two new D_{AB} values for nitrogen–ethylene and nitrogen–butane systems (see Table 3).

In the same year, Hargrove and Sawyer [25] published D_{AB} values of liquid carrier gas pairs at room temperature. In order to overcome the difficulty due to solute’s vapor tension to adsorb to the tubing walls at 298 K, they added a constant amount of the solute to the carrier gas, thereby saturating the adsorption sites. They used the Golay equation (see Section 2.2.2) for the calculation of D_{AB} and a commercial gas chromatograph with syringe injection of vapor samples for their experiments.

Two new chromatographic methods for measuring diffusion coefficients proposed by Zhukhovitskii et al. [26]. In the first method, saturation of a capillary column with helium is followed by connection of the capillary to another tube in which nitrogen is flowing. The estimation of D_{AB} is

Table 3
Binary gaseous diffusion coefficients, D_{AB} ($cm^2\,s^{-1}$) (A: trace solute, B: carrier gas), measured by the chromatographic broadening techniques

Binary system A–B	T (K)	p (atm)	D_{AB} ($cm^2\,s^{-1}$)	Precision[a] (%)	Accuracy[b] (%)	Reference
CH_4–H_2	298.0	1	0.73	2.7	0	[16]
C_2H_6–H_2	298.0	1	0.54	1.9	1.9	[16]
C_3H_8–H_2	298.0	1	0.44	6.8	2.2	[16]
C_4H_{10}–H_2	298.0	1	0.40	3.8	–	[16]
N_2–H_2	298.0	1	0.78	2.6	0	[16]
CH_3OH–H_2	353.0	1	0.9370	1	–	[30]
	373.0	1	1.0200	4.6	–	[30]
	393.0	1	1.1420	4.2	–	[30]
	423.0	1	1.2483	6.8	–	[30]
C_2H_5OH–H_2	353.0	1	0.7200	1.4	–	[30]
	373.0	1	0.7820	1.3	–	[30]
	393.0	1	0.8420	0.61	–	[30]
	423.0	1	0.9460	2.8	–	[30]
	453.0	1	1.0770	4.9	–	[30]
1-Butanol–H_2	373.0	1	0.6479	–	–	[30]
	393.0	1	0.7110	3.2	–	[30]
	423.0	1	0.7983	2.2	–	[30]
	453.0	1	0.9097	4.0	–	[30]
	483.0	1	1.0240	5.4	–	[30]
2-Butanol–H_2	373.0	1	0.6290	–	–	[30]
	393.0	1	0.6760	1.6	–	[30]
	423.0	1	0.7850	3.9	–	[30]
	453.0	1	0.8730	3.9	–	[30]
	483.0	1	0.9690	0.63	–	[30]
n-C_5H_{12}–H_2	353.0	1	0.4895	1.5	–	[30]
	373.0	1	0.5324	3.9	–	[30]
	393.0	1	0.5830	4.3	–	[30]
	423.0	1	0.6300	0.06	–	[30]
	453.0	1	0.7425	0.47	–	[30]
n-C_6H_{14}–H_2	353.0	1	0.4990	0.94	–	[30]
	373.0	1	0.4740	1.5	10	[30]
	393.0	1	0.5310	0.38	–	[30]
	423.0	1	0.5923	0.30	–	[30]
	453.0	1	0.6520	0.0	–	[30]
Cyclohexane–H_2	373.0	1	0.5140	2.5	7.9	[30]
	393.0	1	0.5960	0.67	–	[30]
	423.0	1	0.6742	1.6	–	[30]
	453.0	1	0.7818	2.7	–	[30]
Benzene–H_2	373.0	1	0.5840	1.5	6.4	[30]
	393.0	1	0.6500	2.2	–	[30]
	423.0	1	0.7410	1.1	–	[30]
	453.0	1	0.8220	2.2	–	[30]
	483.0	1	0.8940	0.94	–	[30]
Toluene–H_2	373.0	1	0.5834	–	–	[30]
	393.0	1	0.6170	7.7	–	[30]
	423.0	1	0.6724	0.74	–	[30]
	453.0	1	0.7440	1.5	–	[30]
	483.0	1	0.8197	4.9	–	[30]
H_2–He	289.0	1	1.132	3.4	20	[17]
^{3}He–He	303.0	1	1.88	4.8	3.3	[34]
	403.0	1	3.06	1.3	3.4	[34]
	500.0	1	4.39	1.8	2.1	[34]
	600.0	1	6.08	2.8	4.1	[34]
	698.0	1	7.56	1.9	0.3	[34]
	806.0	1	9.63	3.9	0.2	[34]
N_2–He	77.2	1	0.0725	1.4	–	[28]
	296.0	1	0.678	0.74	–	[28]

Table 3 (*Continued*)

Binary system A–B	T (K)	p (atm)	D_{AB} ($cm^2\ s^{-1}$)	Precision[a] (%)	Accuracy[b] (%)	Reference
	298.0	1	0.687	0.74	0.15	[17]
	298.0	1	0.687	0.87	–	[19]
	303.0	1	0.750	0.93	5.2	[34]
	321.0	1	0.8171	0.61	–	[28]
	323.0	1	0.766	1	–	[19]
	324.0	1	0.798	2.3	3.6	[34]
	343.0	1	0.837	2.6	1.4	[35]
	348.0	1	0.9251	0.76	–	[28]
	353.0	1	0.893	0.56	–	[19]
	370.0	1	1.0300	0.58	–	[28]
	383.0	1	1.077	1.9	–	[19]
	403.0	1	1.13	1.8	2.7	[34]
	413.0	1	1.200	1.6	–	[19]
	443.0	1	1.289	1.1	–	[19]
	473.0	1	1.569	0.45	–	[19]
	498.0	1	1.650	1.3	–	[19]
	500.0	1	1.65	1.2	1.2	[34]
	600.0	1	2.20	0.91	4.1	[34]
	698.0	1	2.81	0.71	5.3	[34]
	806.0	1	3.75	2.4	1.4	[34]
	248.0	9.97	0.0522	–	–	[32]
	248.0	29.9	0.0177	–	–	[32]
	248.0	49.8	0.0107	–	–	[32]
	248.0	59.8	0.00889	–	–	[32]
	273.0	9.97	0.0607	–	–	[32]
	273.0	29.9	0.0206	–	–	[32]
	273.0	49.8	0.0124	–	–	[32]
	273.0	59.8	0.0105	–	–	[32]
	323.0	9.97	0.0820	–	–	[32]
	323.0	29.9	0.0272	–	–	[32]
	323.0	49.8	0.0166	–	–	[32]
	323.0	59.8	0.0140	–	–	[32]
O_2–He	298.0	1	0.718	1.3	–	[17]
	298.0	1	0.729	1.4	–	[19]
	298.0	1	0.7361	0.68	–	[28]
	320.0	1	0.8472	0.71	–	[28]
	323.0	1	0.809	0.87	–	[19]
	353.0	1	0.987	0.30	–	[19]
	365.0	1	1.041	0.77	–	[28]
	383.0	1	1.120	1.4	–	[19]
	413.0	1	1.245	1.1	–	[19]
	443.0	1	1.420	0.56	–	[19]
	473.0	1	1.595	1.6	–	[19]
	498.0	1	1.683	1.1	–	[19]
Ar–He	77.2	1	0.0710	1.3	–	[28]
	296.0	1	0.729	1.0	0.55	[17]
	298.0	1	0.7335	0.55	–	[28]
	298.0	1	0.729	1.2	–	[19]
	303.0	1	0.784	1.0	1.8	[34]
	323.0	1	0.809	1.2	–	[19]
	324.0	1	0.847	1.8	1.9	[34]
	334.0	1	0.8890	0.67	–	[28]
	353.0	1	0.978	1.0	–	[19]
	357.0	1	0.9917	0.61	–	[28]
	383.0	1	1.122	1.2	–	[19]
	413.0	1	1.237	1.1	–	[19]
	402.0	1	1.22	3.3	3.3	[34]
	443.0	1	1.401	1.4	–	[19]
	473.0	1	1.612	0.8	–	[19]
	498.0	1	1.728	1.3	–	[19]
	500.0	1	1.75	1.1	4.6	[34]
	600.0	1	2.52	1.6	0.4	[34]
	698.0	1	3.05	4.6	6.9	[34]

Table 3 (*Continued*)

Binary system A–B	T (K)	p (atm)	D_{AB} ($cm^2\ s^{-1}$)	Precision[a] (%)	Accuracy[b] (%)	Reference
	806.0	1	4.05	2.5	3.5	[34]
	248.0	9.97	0.0541	–	–	[32]
	248.0	29.9	0.0184	–	–	[32]
	248.0	49.8	0.0111	–	–	[32]
	248.0	59.8	0.0937	–	–	[32]
	273.0	9.97	0.0634	–	–	[32]
	273.0	29.9	0.0215	–	–	[32]
	273.0	49.8	0.0130	–	–	[32]
	273.0	59.8	0.0109	–	–	[32]
	298.0	9.97	0.0742	–	–	[32]
	298.0	29.9	0.0249	–	–	[32]
	298.0	49.8	0.0152	–	–	[32]
	298.0	59.8	0.0127	–	–	[31]
	323.0	9.97	0.0851	–	–	[32]
	323.0	29.9	0.0288	–	–	[32]
	323.0	49.8	0.0175	–	–	[32]
	323.0	59.8	0.0145	–	–	[32]
Kr–He	298.0	1	0.6491	0.62	–	[28]
	322.0	1	0.7372	0.54	–	[28]
	341.0	1	0.813	0.62	–	[28]
	366.0	1	0.904	0.66	–	[28]
CH_4–He	298.0	1	0.6776	0.22	–	[37]
	298.0	1	0.6735	0.12	–	[37]
	373.0	1	1.005	–	–	[21]
	373.0	1	1.007	–	–	[36]
	248.0	9.97	0.0501	–	–	[32]
	248.0	29.9	0.0169	–	–	[32]
	248.0	49.8	0.0103	–	–	[32]
	248.0	59.8	0.00872	–	–	[32]
	273.0	9.97	0.0588	–	–	[32]
	273.0	29.9	0.0198	–	–	[32]
	273.0	49.8	0.0119	–	–	[32]
	273.0	59.8	0.0101	–	–	[32]
	298.0	9.97	0.0681	–	–	[32]
	298.0	29.9	0.0229	–	–	[32]
	298.0	49.8	0.0139	–	–	[32]
	298.0	59.8	0.0117	–	–	[32]
	323.0	9.97	0.0781	–	–	[32]
	323.0	29.9	0.0265	–	–	[32]
	323.0	49.8	0.0159	–	–	[32]
	323.0	59.8	0.0134	–	–	[32]
n-C_4H_{10}–He	298.0	1	0.364	0.27	–	[25]
	372.6	1	0.477	2.1	–	[25]
	423.0	1	0.634	0.95	–	[25]
	473.0	1	0.797	0.75	–	[25]
n-C_5H_{12}–He	298.0	1	0.288	0.35	–	[25]
	372.6	1	0.422	0.71	–	[25]
	423.0	1	0.565	1.2	–	[25]
	473.0	1	0.695	17	–	[25]
n-C_6H_{14}–He	298.0	1	0.27	1.8	–	[25]
	372.6	1	0.390	1.5	–	[25]
	417.0	1	0.574	–	–	[21]
	423.0	1	0.513	2.5	–	[25]
	473.0	1	0.629	1.9	–	[25]
n-C_8H_{18}–He	373.0	1	0.3161	1.0	–	[36]
3-Methylheptane–He	373.0	1	0.3334	0.27	–	[36]
2,4-Dimethylhexane–He	373.0	1	0.3340	0.24	–	[36]
3-Ethylhexane–He	373.0	1	0.3363	0.21	–	[36]
2,3-Dimethylhexane–He	373.0	1	0.3420	0.18	–	[36]
3-Ethyl-2-methyl–pentane–He	373.0	1	0.3398	0.12	–	[36]
2,2,4-Trimethylpentane–He	373.0	1	0.3455	0.32	–	[36]

Table 3 (*Continued*)

Binary system A–B	T (K)	p (atm)	D_{AB} ($cm^2\ s^{-1}$)	Precision[a] (%)	Accuracy[b] (%)	Reference
CH_3OH–He	423.0	1	1.032	2.1	–	[19]
	443.0	1	1.135	1.7	–	[19]
	463.0	1	1.218	1.7	–	[19]
	483.0	1	1.335	2.7	–	[19]
	503.0	1	1.389	1.1	–	[19]
	523.0	1	1.475	0.61	–	[19]
C_2H_5OH–He	298.0	1	0.496	–	0.40	[19]
	423.0	1	0.821	1.1	–	[19]
	443.0	1	0.862	1.2	–	[19]
	463.0	1	0.925	1.6	–	[19]
	483.0	1	0.997	3.1	–	[19]
	503.0	1	1.048	0.48	–	[19]
	523.0	1	1.173	0.34	–	[19]
1-Propanol–He	423.0	1	0.676	2.4	–	[19]
	443.0	1	0.711	0.98	–	[19]
	463.0	1	0.761	2.4	–	[19]
	483.0	1	0.829	0.56	–	[19]
	503.0	1	0.896	0.60	–	[19]
	523.0	1	0.959	0.10	–	[19]
2-Propanol–He	423.0	1	0.677	3.2	–	[19]
	443.0	1	0.732	0.68	–	[19]
	463.0	1	0.784	0.77	–	[19]
	483.0	1	0.834	1.3	–	[19]
	503.0	1	0.882	0.68	–	[19]
	523.0	1	0.988	2.0	–	[19]
1-Butanol–He	423.0	1	0.587	1.9	–	[19]
	443.0	1	0.653	0.92	–	[19]
	463.0	1	0.689	0.87	–	[19]
	483.0	1	0.746	0.80	–	[19]
	503.0	1	0.792	1.1	–	[19]
	523.0	1	0.841	0.12	–	[19]
1-Pentanol–He	423.0	1	0.507	0.99	–	[19]
	443.0	1	0.536	0.75	–	[19]
	463.0	1	0.578	2.2	–	[19]
	483.0	1	0.636	1.1	–	[19]
	503.0	1	0.666	0.75	–	[19]
	523.0	1	0.729	0.96	–	[19]
1-Hexanol–He	423.0	1	0.469	1.5	–	[19]
	443.0	1	0.496	1.4	–	[19]
	463.0	1	0.531	0.19	–	[19]
	483.0	1	0.584	2.1	–	[19]
	503.0	1	0.631	0.63	–	[19]
	523.0	1	0.686	0.44	–	[19]
Ether–He	298.0	1	0.310	0.32	–	[25]
	372.6	1	0.460	2.2	–	[25]
	423.0	1	0.607	1.3	–	[25]
	473.0	1	0.745	3.9	–	[25]
Acetone–He	298.0	1	0.411	3.4	–	[25]
	372.6	1	0.638	2.7	–	[25]
	423.0	1	0.754	1.9	–	[25]
	473.0	1	0.889	1.9	–	[25]
Benzene–He	298.0	1	0.367	2.5	–	[25]
	372.6	1	0.498	3.6	–	[25]
	423.0	1	0.614	0.16	–	[25]
	423.0	1	0.610	0.33	–	[19]
	446.0	1	0.662	0.15	–	[19]
	463.0	1	0.715	0.42	–	[19]
	473.0	1	0.778	2.1	–	[25]
	483.0	1	0.766	1.6	–	[19]

Table 3 (*Continued*)

Binary system A–B	T (K)	p (atm)	D_{AB} ($cm^2\ s^{-1}$)	Precision[a] (%)	Accuracy[b] (%)	Reference
	503.0	1	0.815	1.5	–	[19]
	523.0	1	0.861	0.12	–	[19]
CH_2F_2–He	430.8	1	0.874	3.4	–	[5]
$C_2H_4F_2$–He	429.6	1	0.754	2.0	–	[5]
1-Fluorohexane–He	431.6	1	0.492	1.2	–	[5]
Fluorobenzene–He	429.7	1	0.566	1.4	–	[5]
C_6F_6–He	428.7	1	0.453	1.8	–	[5]
4-Fluorotoluene–He	431.6	1	0.508	1.2	–	[5]
CH_2Cl_2–He	427.5	1	0.750	1.2	–	[5]
$CHCl_3$–He	429.1	1	0.624	1.9	–	[5]
$C_2H_4Cl_2$–He	427.1	1	0.683	0.88	–	[5]
1-Chloropropane–He	427.5	1	0.631	1.4	–	[5]
1-Chlorobutane–He	429.2	1	0.555	1.8	–	[5]
2-Chlorobutane–He	429.1	1	0.561	1.4	–	[5]
1-Chloropentane–He	428.2	1	0.518	0.77	–	[5]
Chlorobenzene–He	430.9	1	0.542	1.1	–	[5]
Dibromomethane–He	427.7	1	0.665	1.1	–	[5]
Bromoethane–He	427.7	1	0.740	1.5	–	[5]
1-Bromopropane–He	428.2	1	0.592	1.5	–	[5]
2-Bromopropane–He	428.0	1	0.606	2.0	–	[5]
1-Bromobutane–He	426.6	1	0.545	1.1	–	[5]
2-Bromobutane–He	427.2	1	0.553	2.4	–	[5]
1-Bromohexane–He	427.5	1	0.461	1.7	–	[5]
2-Bromohexane–He	427.9	1	0.470	2.6	–	[5]
3-Bromohexane–He	428.5	1	0.469	0.85	–	[5]
Bromobenzene–He	427.1	1	0.543	1.8	–	[5]
2-Bromo-1-chloropropane–He	427.2	1	0.570	2.8	–	[5]
Iodomethane–He	431.2	1	0.783	2.0	–	[5]
Iodoethane–He	428.4	1	0.648	2.0	–	[5]
1-Iodopropane–He	430.0	1	0.579	1.2	–	[5]
2-Iodopropane–He	430.2	1	0.579	2.1	–	[5]
1-Iodobutane–He	428.1	1	0.524	1.3	–	[5]
2-Iodobutane–He	427.1	1	0.545	2.4	–	[5]
NH_3–He	297.0	0.84	0.923	0.76	–	[17]
CO_2–He	298.0	1	0.612	0.49	–	[19]
	323.0	1	0.678	1.8	–	[19]
	353.0	1	0.800	1.6	–	[19]
	383.0	1	0.884	0.90	–	[19]
	413.0	1	1.040	1.1	–	[19]
	443.0	1	1.133	1.6	–	[19]
	473.0	1	1.279	1.5	–	[19]
	498.0	1	1.414	2.0	–	[19]
	248.0	9.97	0.0454	–	–	[32]
	248.0	29.9	0.0151	–	–	[32]
	248.0	39.8	0.0116	–	–	[32]
	248.0	49.8	0.00920	–	–	[32]
	273.0	9.97	0.0525	–	–	[32]
	273.0	29.9	0.0177	–	–	[32]
	273.0	39.8	0.0133	–	–	[32]
	273.0	49.8	0.0107	–	–	[32]
	298.0	9.97	0.0616	–	–	[32]
	298.0	29.9	0.0206	–	–	[32]
	298.0	39.8	0.0156	–	–	[32]
	298.0	49.8	0.0127	–	–	[32]
	323.0	9.97	0.0701	–	–	[32]
	323.0	29.9	0.0236	–	–	[32]
	323.0	39.8	0.0177	–	–	[32]
	323.0	49.8	0.0141	–	–	[32]
H_2–N_2	273.0	1	0.687	2.0	0.58	[17]
	293.0	1	0.7975	1.9	4.	[8]
	324.0	1	0.876	–	3.6	[15]

Table 3 (*Continued*)

Binary system A–B	T (K)	p (atm)	D_{AB} ($cm^2\ s^{-1}$)	Precision[a] (%)	Accuracy[b] (%)	Reference
He–N_2	293.0	1	0.605	3.6	–	[26]
	298.0	1	0.717	0.86	1.8	[17]
	310.2	1	0.784	–	–	[33]
	315.2	1	0.812	–	–	[33]
	323.2	1	0.858	–	–	[33]
	330.2	1	0.867	–	–	[33]
	334.4	1	0.898	–	–	[33]
	340.2	1	0.927	–	–	[33]
	346.2	1	0.948	–	–	[33]
	353.9	1	0.978	–	–	[33]
	394.5	1	1.025	–	–	[33]
O_2–N_2	298.0	1	0.23	–	4.3	[23]
	324.0	1	0.258	–	6.6	[15]
H_2O–N_2	393.2	1	0.441	–	–	[33]
	408.2	1	0.464	–	–	[33]
	423.4	1	0.508	–	–	[33]
CO_2–N_2	298.0	1	0.163	0.52	2.4	[17]
	324.0	1	0.186	–	4.1	[15]
C_2H_6–N_2	298.0	1	0.14	18	–	[16]
C_3H_8–N_2	298.0	1	0.11	–	–	[16]
n-C_4H_{10}–N_2	298.0	1	<0.07	–	–	[16]
	298.0	1	0.0954	–	0.63	[25]
	302.4	1	0.100	–	1.5	[24]
n-C_5H_{12}–N_2	353.0	1	0.136	–	–	[31]
C_2H_4–N_2	291.0	0.99	0.165	0.61	–	[20]
	291.0	1	0.160	–	–	[18]
	302.6	1	0.170	–	2.4	[24]
$C_2H_2Cl_4$–N_2	423.0	1	0.143	–	–	[39]
$CHCl_3$–N_2	361.0	1	0.135	–	–	[33]
	373.0	1	0.140	–	–	[39]
	383.2	1	0.143	–	–	[33]
	403.2	1	0.161	–	–	[33]
	418.2	1	0.173	–	–	[33]
CCl_4–N_2	363.7	1	0.113	–	–	[33]
	373.0	1	0.120	–	–	[39]
	383.2	1	0.124	–	–	[33]
	403.2	1	0.134	–	–	[33]
	423.2	1	0.147	–	–	[33]
CH_3OH–N_2	355.0	1	0.250	–	10	[31]
1-Propanol–N_2	373.0	1	0.153	–	–	[39]
2-Propanol–N_2	357.0	1	0.146	–	3.5	[31]
	362.9	1	0.159	–	–	[33]
	383.2	1	0.168	–	–	[33]
1-Butanol–N_2	393.0	1	0.161	–	–	[39]
1-Pentanol–N_2	418.0	1	0.159	–	–	[39]
1-Hexanol–N_2	433.0	1	0.141	–	–	[39]
1-Heptanol–N_2	453.0	1	0.145	–	–	[39]
1-Octanol–N_2	473.0	1	0.148	–	–	[39]
Acetone–N_2	343.1	1	0.140	–	–	[33]
	353.0	1	0.135	–	5.2	[31]
	363.3	1	0.154	–	–	[33]
	373.0	1	0.168	–	–	[39]
	383.2	1	0.170	–	–	[33]
Methyl acetate–N_2	357.0	1	0.168	–	14	[31]
	363.5	1	0.171	–	–	[33]
	383.1	1	0.192	–	–	[33]
	403.8	1	0.209	–	–	[33]

Table 3 (*Continued*)

Binary system A–B	T (K)	p (atm)	D_{AB} ($cm^2\ s^{-1}$)	Precision[a] (%)	Accuracy[b] (%)	Reference
Ethyl formate–N_2	343.7	1	0.131	–	–	[33]
Ethyl acetate–N_2	355.0	1	0.137	–	12	[31]
Ethyl formate–N_2	363.2	1	0.143	–	–	[33]
	383.2	1	0.158	–	–	[33]
	403.2	1	0.168	–	–	[33]
Methyl isobutyl ketone–N_2	423.0	1	0.141	–	–	[39]
Cyclohexane–N_2	363.2	1	0.124	–	–	[33]
	383.2	1	0.134	–	–	[33]
	403.2	1	0.149	–	–	[33]
Benzene–N_2	353.0	1	0.133	–	2.2	[31]
	364.2	1	0.129	–	–	[33]
	378.2	1	0.140	–	–	[33]
	393.4	1	0.154	–	–	[33]
	403.2	1	0.163	–	–	[33]
	423.2	1	0.165	–	–	[33]
Nitrobenzene–N_2	523.0	1	0.225	–	–	[39]
Chlorobenzene–N_2	423.0	1	0.65	–	–	[39]
Bromobenzene–N_2	473.0	1	0.173	–	–	[39]
o-Nitrotuluene–N_2	498.0	1	0.170	–	–	[39]
He–O_2	298.0	1	0.737	0.58	–	[17]
n-C_4H_{10}–Ar	298.0	1	0.104	3.8	–	[25]
	372.6	1	0.139	2.2	–	[25]
	423.0	1	0.170	1.8	–	[25]
	473.0	1	0.209	2.9	–	[25]
n-C_5H_{12}–Ar	298.0	1	0.0890	0.90	–	[25]
	372.6	1	0.115	7.8	–	[25]
	423.0	1	0.149	2.0	–	[25]
	473.0	1	0.186	2.2	–	[25]
n-C_6H_{14}–Ar	293.0	1	0.0845	3.3	–	[25]
	372.6	1	0.107	0.93	–	[25]
	423.0	1	0.145	2.1	–	[25]
	473.0	1	0.175	2.9	–	[25]
Benzene–Ar	298.0	1	0.108	0.93	–	[25]
	372.6	1	0.142	1.4	–	[25]
	423.0	1	0.169	0.59	–	[25]
	473.0	1	0.212	1.4	–	[25]
Acetone–Ar	298.0	1	0.115	2.6	–	[25]
	372.6	1	0.175	1.7	–	[25]
	423.0	1	0.213	0.94	–	[25]
	473.0	1	0.249	1.2	–	[25]
Ether–Ar	298.0	1	0.0849	1.99	–	[25]
	372.6	1	0.116	2.6	–	[25]
	423.0	1	0.165	1.8	–	[25]
	473.0	1	0.203	3.9	–	[25]
H_2–CO_2	298.0	1	0.665	0.38	4.1	[17]
He–CO_2	313.8	1	0.633	–	–	[33]
	324.3	1	0.668	–	–	[33]
	332.3	1	0.720	–	–	[33]
	342.3	1	0.746	–	–	[33]
	353.1	1	0.794	–	–	[33]
	364.5	1	0.816	–	–	[33]
N_2–CO_2	298.0	1	0.181	1.4	8.4	[33]
	313.7	1	0.201	–	–	[33]
	323.2	1	0.209	–	–	[33]
	332.6	1	0.232	–	–	[33]
	342.6	1	0.238	–	–	[33]
	354.2	1	0.251	–	–	[33]

Table 3 (*Continued*)

Binary system A–B	T (K)	p (atm)	D_{AB} ($cm^2\ s^{-1}$)	Precision[a] (%)	Accuracy[b] (%)	Reference
	365.1	1	0.269	–	–	[33]
H_2O–CO_2	393.8	1	0.297	–	–	[33]
	408.5	1	0.311	–	–	[33]
	423.3	1	0.333	–	–	[33]
2-Propanol–CO_2	362.8	1	0.110	–	–	[33]
	383.5	1	0.120	–	–	[33]
	403.3	1	0.135	–	–	[33]
	418.1	1	0.145	–	–	[33]
Methyl acetate–CO_2	363.2	1	0.114	–	–	[33]
	383.2	1	0.126	–	–	[33]
Ethyl formate–CO_2	333.5	1	0.099	–	–	[33]
	348.3	1	0.105	–	–	[33]
	362.9	1	0.116	–	–	[33]
Cyclohexane–CO_2	363.1	1	0.098	–	–	[33]
	383.0	1	0.108	–	–	[33]
	403.4	1	0.114	–	–	[33]
	423.4	1	0.126	–	–	[33]
Benzene–CO_2	363.6	1	0.105	–	–	[33]
	378.0	1	0.116	–	–	[33]
	393.7	1	0.122	–	–	[33]
	408.2	1	0.130	–	–	[33]
	422.8	1	0.150	–	–	[33]
CCl_4–CO_2	363.3	1	0.085	–	–	[33]
	384.3	1	0.093	–	–	[33]
	403.1	1	0.100	–	–	[33]
	423.0	1	0.111	–	–	[33]
$CHCl_3$–CO_2	363.3	1	0.110	–	–	[33]
	383.3	1	0.120	–	–	[33]
	403.8	1	0.129	–	–	[33]
CO_2–CH_4	298.0	1	0.17	18	5.6	[16]
CH_3T–CH_4	298.0	2.04	0.106	–	–	[32]
	298.0	6.78	0.0319	–	–	[32]
	298.0	20.4	0.0100	–	–	[32]
	298.0	33.9	0.00598	–	–	[32]
	298.0	47.5	0.00429	–	–	[32]
	298.0	61.1	0.00323	–	–	[32]
CH_3T–CF_4	298.0	2.05	0.0688	–	–	[32]
	298.0	6.78	0.0204	–	–	[32]
	298.0	20.4	0.00643	–	–	[32]
	298.0	33.9	0.00373	–	–	[32]
	298.0	47.5	0.00240	–	–	[32]
	298.0	61.1	0.00177	–	–	[32]

[a] Precision as given by the authors. Otherwise precision has been defined as $100 \times \text{deviation}/D_{AB}$.
[b] Accuracy as given by the authors. Otherwise accuracy has been defined as $100 \times |D_{AB} - D_{lit}|/D_{AB}$.

done by Golay equation. The main disadvantage of the technique is the extremely long analysis time (20–40 h). In their second method, a sample of weakly sorbed gas was allowed to diffuse into a carbon packed column.

In 1969, Fuller et al. [5] published a paper in which the diffusion characteristics of halogenated hydrocarbons in helium were studied. They improved the experimental apparatus by using a more spacious oven, permitting the use of a large coil diameter column, and hence less distortion of the sample profile was achieved. They also eliminated the use of the short corrector (second) column by using a gas-sampling valve permitting direct on column injection and a flame ionization detector with a minimum dead volume. By using the above mentioned improved methodology they measured the diffusion coefficients for 31 halogenated hydrocarbons into helium (29 were for new binary gas systems). The relative standard deviation of their work for most systems was about 2%. However, the most important result of this publication is the measurement of collision cross-sections by using binary diffusion coefficients. What was previously known about collision cross-sections was determined mainly from viscosity data. Binary diffusion coefficient measurement provides

a direct measurement of the interaction between dissimilar molecules. The authors argue that, the use of helium as one member of the diffusing pair, gives a sensitive probe into the cross-section of a much larger molecule.

Balenovic et al. [27] modified the apparatus used in [5], because of the extremely high pressures involved with diffusion measurements at pressures up to 1360 atm, where the density approaches that of a liquid. The equipment was modified in order to measure diffusion coefficients of dense gases. This work indicates the versatility of GC approach to D_{AB} measurements.

Wasik and McCulloh [28] solved the problem of finite injection volume by allowing the solute to pass through a column and a detector directly into the diffusion column and a second detector. They also developed equations describing the additional peak broadening in the second column. A disadvantage of their modification is that the measurement time is doubled, and the existence of a slight distortion of the peak caused by its passage through the first detector.

Another method based on frontal analysis was developed by Lozgachev and Kancheeva [29]. Unfortunately, their method suffered from rather poor precision, about 20% for a three-component mixture. Extensive diffusion coefficient measurements by other GC methods were also done in the same period [30–34].

Huang et al. [6] studied the effect of temperature and pressure on gaseous diffusion. They also presented an equation for estimating D_{AB} from known molar volumes V_A and V_B and molecular weights M_A and M_B, the pressure p, the temperature T, and a correlation factor A. They found the temperature dependence of $D_{AB} \propto T^{1.75}$, which is in agreement with the results of Fuller et al. [21], but they also found that in the pressure range of 750 to about 1700 mmHg the pressure dependence of $D_{AB} \propto p^{1.286}$, in contrast with the assumption of the most workers about a simple inverse pressure dependence. The average error in that method was 3.5%.

Grushka and Maynard [35] used the GC technique in an instrumental analysis course, demonstrating both chromatographic theories and measurement of physicochemical parameters. Their presented results had a precision of about 5%.

Grushka and Maynard [36] using the GC continuous elution method determined the diffusion coefficients of seven octane isomers in helium in order to investigate the effect of molecular geometries. They built an extremely precise chromatographic system, incorporating a fast-switching injection valve, precise temperature control (±0.1 °C) and computer data reduction. The diffusion coefficients were calculated from the variances of Gaussian peaks, which were least-square fitted to the actual data. The least precise results had a relative standard deviation of about 1%, while the overall relative standard deviation was about 0.34%. They also found a linear dependence of D_{AB} on critical volume, and modified the FSG equation [4,21] to allow for estimation of isomers.

Another important work was published in 1976 by Young et al. [37]. A specially designed gas chromatograph was tested for the measurement of the diffusion coefficient of methane in helium at 25 °C. Both the continuous elution and Knox's arrested elution techniques were used. They also employed a computer for accurate data collection and for least-squares fitting of the theoretical zone dispersion equation. The authors state that the advantage of both the continuous and arrested elution methods may only be appreciated if a single run of the experiment will be sufficient for the measurement of a D_{AB} value with high precision and accuracy. This was achieved by a direct least-squares fit of the experimental data to a theoretical equation of the eluted concentration profile and computing the best D_{AB} value. Their approach may be adopted either to the arrested elution method or to the continuous elution method. Another advantage of their approach is that any deviation from the expected form of the concentration profiles gives warning of incorrect design of the experiment or malfunction of the equipment. They also found that more reliable is the arrested elution technique.

Most of the techniques based on chromatography have been reviewed by Choudhary [38]. Several other studies have also been reported [39–45] using the arrested elution method of Knox for the measurement of diffusion coefficients.

After the above historical review of the gas chromatographic broadening techniques used till now for the measurement of gaseous diffusivity, it is shown that the Giddings continuous elution and Knox's arrested elution techniques are the most important ones and the following presentation of the theoretical and experimental information will be focused on these two techniques.

2.2.2. Theoretical part

2.2.2.1. Mass-balance equation. The mass-balance equation that applies for the diffusion of a trace amount of a solute in an open tube containing a flowing solvent is:

$$\frac{\partial c}{\partial t} - D_{AB} \cdot \left[\frac{\partial^2 c}{\partial x^2} + \frac{1}{r} \cdot \frac{\partial}{\partial r} \left(r \cdot \frac{\partial c}{\partial r} \right) \right] + 2\bar{\upsilon} \cdot \left[1 - \left(\frac{r}{r_0} \right) \right]^2 \cdot \frac{\partial c}{\partial x} = 0 \quad (9)$$

where D_{AB} is the binary diffusion coefficient of the solute–solvent pair, c is the concentration, t is the time, x is the longitudinal coordinate of the tube, r is the radial coordinate of the tube, r_0 is the radius of the tube and $\bar{\upsilon}$ is the average carrier gas velocity. To solve the mass-balance equation, the establishment of boundary conditions and simplifying assumptions is necessary: (a) the solute cannot pass through the tubing wall, (b) the radial concentration gradient is zero at the center of the tube, (c) the introduction of the solute is a delta (δ) function, (d) the solute does not interact with the wall, (e) the ratio of solute–wall to solute–solvent collisions is small, and (f) there is no

turbulence and the flow is laminar. Under these boundary conditions and simplifying assumptions, Eq. (9) can be solved to give the analytical form of the concentration profile, which describes a Gaussian distribution with variance σ^2:

$$\sigma^2 = \frac{2D_{AB}L}{\bar{\upsilon}} + \frac{r_0^2\bar{\upsilon}L}{24D_{AB}} \quad (10)$$

from which the plate height H, is obtained.

$$H = \frac{2D_{AB}}{\bar{\upsilon}} + \frac{r_0^2\bar{\upsilon}}{24D_{AB}} \quad (11)$$

2.2.2.2. Golay equation. An alternative equation describing band broadening in coated-open-tube columns is the Golay equation [1,9]:

$$H = \frac{2D_{AB}}{\bar{\upsilon}} + \frac{2R(1-R)}{3}\cdot\frac{d_f^2\bar{\upsilon}}{D_L} + \frac{(11-16R+6R^2)r_0^2\bar{\upsilon}}{24D_{AB}} \quad (12)$$

In Eq. (12), d_f is the thickness of the stationary-phase film coated on the tube, D_L the diffusion coefficient of the solute in the stationary phase and R is the ratio of the solute velocity to the carrier gas velocity. In the case where there is no coating on the tube (which is concerned here) $d_f = 0$ and there is no retention of the solute ($R = 1$), the Golay equation reduces to Eq. (11). Rearranging Eq. (11) yields:

$$D_{AB} = \frac{\bar{\upsilon}}{4}\cdot\left[H \pm \left(H^2 - \frac{r_0^2}{3}\right)^{1/2}\right] \quad (13)$$

From the two values given by Eq. (13) for the diffusion coefficient only one is meaningful. When the flow velocity is slow the second term of Eq. (11) is small and the determination of D_{AB} is done from the positive root. At higher flow velocities the first term of Eq. (11) is small and the negative root is used for the calculation of the diffusion coefficient. The value of $\bar{\upsilon}_{opt}$ which minimizes H is found by differentiating Eq. (11) with respect to $\bar{\upsilon}$, and setting the answer equal to zero. The result is:

$$\bar{\upsilon}_{opt} = \frac{(48D_{AB})^{1/2}}{r_0} \quad (14)$$

To solve the above equation, knowledge of r, $\bar{\upsilon}$ and H is necessary. The value of r_0 can be measured directly and $\bar{\upsilon}$ can be found by dividing tube's length, L, by the retention time of the solute, t_R. Both L and t_R can be measured directly. The plate height H can be obtained experimentally.

2.2.3. Experimental

2.2.3.1. Continuous elution method. The continuous elution method for the determination of D_{AB} is generally conducted in an open tube with circular cross-section. It uses a commercial GC apparatus where the packed column is replaced. The average carrier gas velocity, $\bar{\upsilon}_{opt}$, is chosen such that the plate height is minimized, as described in Section 2.2.2 (see Eq. (14)). The major advantage of the method is that the speed of collecting data is rapid. The speed can even be faster if a shorter column is employed. However the method suffers from the fact that zone broadening factors cannot be isolated in the same run of experiment.

To correct for end effects and for diffusion occurring in the instrument dead volumes, Giddings and Seager [17] introduced the use of two different length columns. All experimental data are taken with both the short and the long tube. The equation for H from which the diffusion coefficient is obtained, by means of Eq. (13), is:

$$H = (L_d - L_c)\cdot\left[\frac{\tau_d^2 - \tau_c^2}{(t_d - t_c)^2}\right] \quad (15)$$

where L_d and L_c are the lengths of the principal (long) and correction (short) columns, respectively, while $(\tau_d^2 - \tau_c^2)$ and $(t_d - t_c)$ are the corresponding differences for the second and first moments of the time base. However identity of two separate sets of experimental conditions (velocity, temperature, sample concentration, etc.) is very difficult to achieve, especially after the exchange of column.

2.2.3.2. Arrested elution method. The experimental setup used by arrested elution method is basically the same as that used by the continuous elution method. Knox and McLaren [20] presented an elution method permitting the determination of gaseous diffusion coefficients, D_{AB} (empty column), as well as obstructive factors, γ (packed column). This method is applicable equally to open or packed columns.

A typical experiment is carried out as follows: a solute sample is injected into the column and eluted in the normal way without arresting the gas flow. From the time of passage along the column, the outlet velocity is obtained. To study static spreading in a particular column a band of solute is eluted about half way along the column at the linear flow-rate used in the continuous elution experiment. The flow is then switched to a dummy column of equal resistance (see Fig. 1 of [20]). After a delay of 1–20 min the flow is reconnected to the column and the peak is eluted. During the delay time the spreading of the band can occur only by diffusion. Finally, the band is eluted and its concentration profile and standard deviation are determined by the detector. Provided that the solute is not sorbed by the column, the following equations hold for the additional variance σ^2 produced by diffusion during the delay period:

$$\frac{d\sigma^2}{dt} = \frac{2D_{AB}}{\bar{\upsilon}^2} \quad \text{(empty tube)} \quad (16)$$

$$\frac{d\sigma^2}{dt} = \frac{2\gamma D_{AB}}{\bar{\upsilon}^2} \quad \text{(packed tube)} \quad (17)$$

The band broadening produced by the injector, column connections, detector, and elution along the column are the same, whatever the delay and can accordingly be subtracted

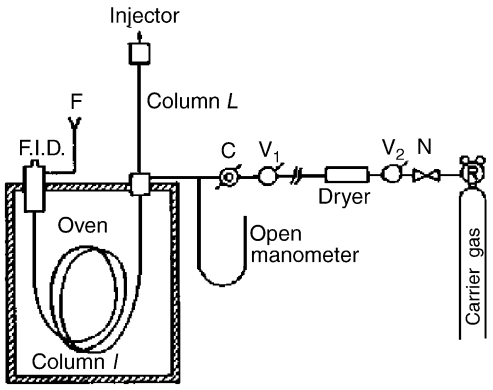

Fig. 1. Gas lines and important connections for determining diffusion coefficients by stopped-flow gas chromatography. R: two-stage reducing valve and pressure regulator; N: needle valve; V_1, V_2: shut-off valves for stopping and restoring carrier gas flow through column *l*; C: gas flow controller; F: bubble flowmeter [47].

out. Thus, a plot of σ^2 against delay should be a straight line of gradient $2D_{AB}/\bar{v}^2$ or $2\gamma D_{AB}/\bar{v}^2$, where $\bar{v}$ is the outlet elution velocity. Since $\bar{v}$ occurs to the second power in Eqs. (16) and (17), its accurate measurement is crucial to the precision of the method. The overall reproducibility of the method is ±2% [20].

The major advantage of using the arrested elution method is that the effects of zone broadening other than axial molecular diffusion and non-uniform flow profile, do not affect the measurement, and therefore, the end effect correction is not necessary. Furthermore, no assumptions are made about the precise form of the flow profile, the smoothness of the column wall, or the accuracy in the knowledge of column diameter. However, the elution arrested method has two drawbacks in comparison with continuous elution method. The first is the need for several runs to get a D_{AB} value with a precision of 2%. The second is the need for constant flow-rates over long periods for runs at various arrested times.

2.2.4. Results

Diffusion coefficients measured by gas chromatographic broadening techniques (continuous, as well as arrested elution methods) are shown in Table 3. The precision, as well as the accuracy as given by the different authors for the different studied systems are also mentioned in Table 3.

2.3. The flow perturbation techniques

Two flow perturbation gas chromatographic techniques are used for the measurement of gaseous diffusion coefficients, namely the stopped-flow and the reversed-flow techniques.

2.3.1. The stopped-flow technique

The stopped-flow technique introduced in 1967 by Phillips et al. for studying the kinetics of surface-catalyzed reactions [46]. It consists in stopping the carrier gas flow for short time intervals, which is most easily done by using shut-off valves. Thus, sophisticated mechanical, pneumatic or other special systems are not required as in flow programming GC.

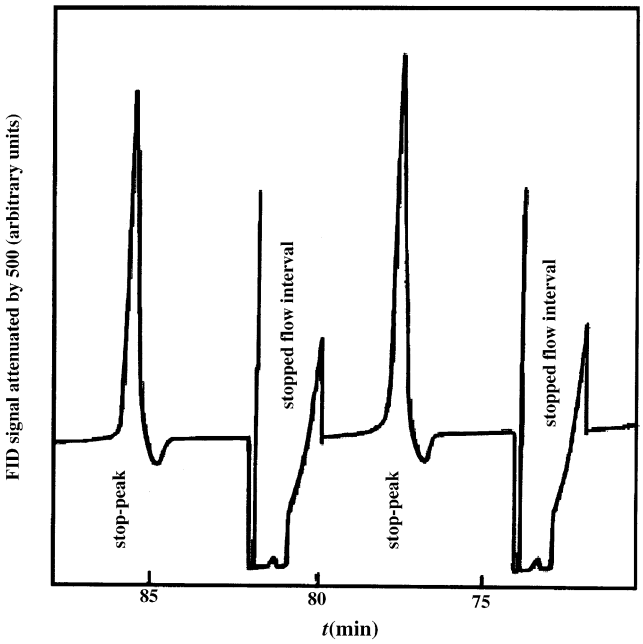

Fig. 2. Stopped-flow chromatogram for measuring diffusion coefficients. Solute was propene and carrier gas nitrogen. $T = 296\,K$, $p = 1\,atm$ [47].

The experimental setup, for measuring gas diffusion coefficients by the stopped-flow GC, is a simple gas chromatograph with an appropriate detector, modified as shown in Fig. 1. Both column sections *L* and *l* are empty of any material and can be thermostated at the same or different temperature. While carrier gas is flowing through the chromatographic column *l*, a small amount of solute (usually $1\,cm^3$ of gas or vapor at atmospheric pressure) is injected into the diffusion column *L*. At known times from the moment of injection the flow of the carrier gas is stopped for a defined time (cf. for 2 min), by simultaneously closing valves V_1 and V_2 (see Fig. 1). Following each restoration of the gas flow, a narrow peak (stop-peak) is recorded in the chromatographic trace (see Fig. 2). The problem to be solved here is to determine the area under the curve of each stop-peak as a function of the time of the corresponding stop in the flow of the carrier gas, under the following assumptions: (i) radial diffusion in the column is negligible, (ii) axial diffusion of solute in the chromatographic column *l* is negligible. This seems reasonable for a high enough flow-rate of the carrier gas, and (iii) the solute is introduced in an "infinitesimally" small section of the diffusion column *L*, so that the feed band can be described by a delta function.

Since the stop-peaks are fairly symmetrical and have a constant half-width, their height from the baseline *H* rather than their area *f* is used to plot $\ln(Ht^{3/2})$ versus the inverse time, $1/t$, according to the following equation produced in

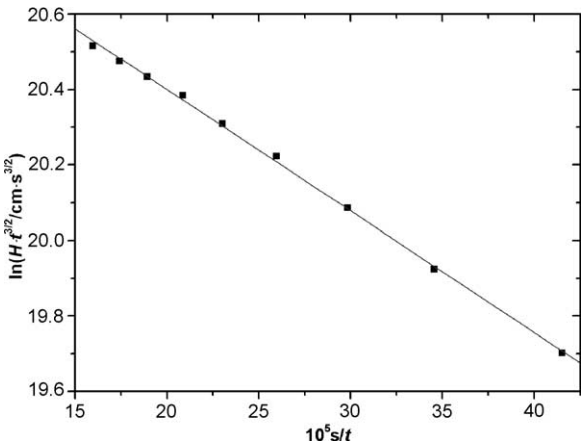

Fig. 3. Plot of Eq. (18) for the diffusion of propene into nitrogen at 296 K and $p = 1$ atm ($L = 40$ cm, $l = 2.7$ m, $\dot{V} = 0.167\,\mathrm{cm^3\,s^{-1}}$) [47].

[47]:

$$\ln(Ht^{3/2}) = \ln\left(\frac{mt_s L}{\pi^{1/2} D_{AB}^{1/2}}\right) - \frac{L^2}{4D_{AB}} \cdot \frac{1}{t} \quad (18)$$

where m is the injected amount of solute in mol, t_s is the stopped-flow interval in s, L is the length of the diffusion column (the column through which carrier gas does not flow) in cm, D_{AB} is the diffusion coefficient of the solute A injected into the carrier gas B ($\mathrm{cm^2\,s^{-1}}$), and t is the time interval from injection of solute to beginning of stopped-flow interval in s.

Eq. (18) permits the calculation of D_{AB} from the slope ($-L^2/4D_{AB}$) of the $\ln(Ht^{3/2})$ plot versus $1/t$. A typical plot of Eq. (18) is shown in Fig. 3, and some representative results are collected in Table 4. It is seen from this table that the differences in the values of D_{AB} determined with varying values of L, l and $\dot{V}$ are not at all statistically significant, and lie within the 95% fiducial limits of the mean value.

One final remark is that the values of diffusion coefficient determined by the stopped-flow GC are very sensitive to the precision with which L is measured, since D_{AB} is proportional to L^2. Instead of measuring L directly, one can use a solute of accurately known diffusion coefficient in the given carrier gas, and carry out a calibration experiment for L. The value of L so determined can now be used, to estimate unknown diffusion coefficients.

Table 4
Diffusion coefficients of three solutes into nitrogen at 296 K and 1 atm, determined by stopped-flow method

Solute	L (cm)	l (cm)	$\dot{V}$ ($\mathrm{cm^3\,s^{-1}}$)	D_{AB} ($\mathrm{cm^2\,s^{-1}}$)
Propene	18	2.7	0.167	0.127[a]
Propene	18	2.7	0.327	0.130
Propene	18	2.7	0.833	0.129
Propene	40	2.7	0.167	0.124
Propene	18	1.5	0.167	0.124
Ethene	18	2.7	0.167	0.186[b]
Diethyl ether	18	2.7	0.167	0.0889[c]
Ether	40	2.7	0.167	0.0927

[a] Mean of seven values having a sample standard deviation 0.003 and 95% fiducial limits 0.127 ± 0.0027.
[b] Literature [48] value is $0.170\,\mathrm{cm^2\,s^{-1}}$.
[c] Literature [48] value in air and 293 K is $0.089\,\mathrm{cm^2\,s^{-1}}$.

2.3.2. The reversed-flow technique

2.3.2.1. Experimental. The reversed-flow GC technique, which was introduced in its preliminary form in 1980 [49], is a tool for physicochemical measurements [50–58] which dismisses the carrier gas from doing the work and "appoints" the gaseous diffusion process in its place. The carrier gas performs only the sampling procedure to measure the gas-phase concentration of an analyte at a certain position of the GC system as a function of time. It is based on reversing the direction of flow of the carrier gas from time-to-time. The experimental setup for the application of the reversed-flow gas chromatography (RF-GC) method is very simple and comprises generally:

(1) A conventional gas chromatograph with any kind of detector capable of detecting the solute(s) contained in the carrier gas.
(2) A so-called sampling column constructed from glass or stainless steel chromatographic tube of any diameter (usually 5.3 mm), and having a total length 0.6–2.0 m, depending on the particular application. The sampling column, which is coiled and accommodated inside the chromatographic oven, should be completely empty of any solid material for the determination of the diffusion coefficient of pure gases into pure gases or mixtures of gases, or it can be filled with a usual chromatographic material for the measurement of the diffusion coefficient of ternary gas mixtures into pure gases.
(3) A diffusion column, which is constructed from the same material with the sampling column, is connected perpendicularly to it, usually at its middle point. The other end of the diffusion column is closed with an injector septum and is used as the injection point of the solute under study. The diffusion column, which is empty of any solid material, is a straight or coiled relatively short (30–80 cm) piece of empty tube placed inside the chromatographic oven.
(4) The sampling and the diffusion column form that we call the sampling cell, and this cell must now be connected to the detector and to the carrier gas inlet in such a way that the carrier gas flow through the sampling column (it is stagnant in the diffusion column) can be reversed in direction by a four-part valve which is connected with the two ends D_1 and D_2 of the chromatographic column, as well as with the inlet of the carrier gas and the detector, as shown in Fig. 4.
(5) In case a detection method with a flame is used (flame ionization detection (FID) or flame photometric detection (FPD)) a restrictor is placed between the valve

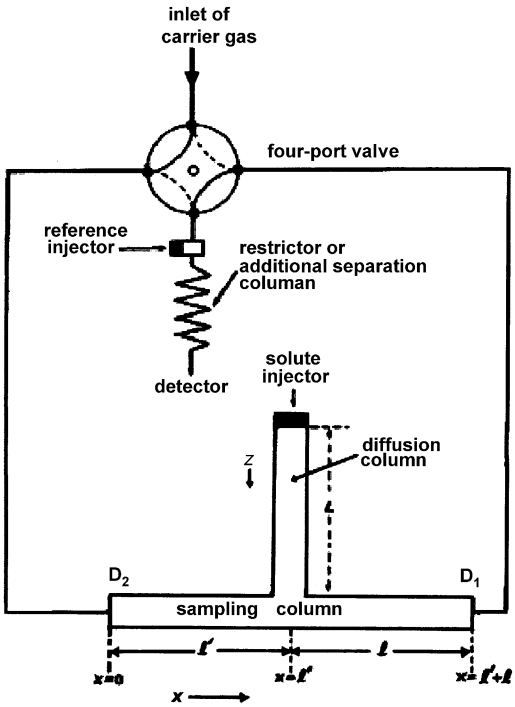

Fig. 4. Schematic representation of the columns and gas connections in the reversed-flow technique [51].

and the detector to prevent the flame from being extinguished when the valve is turned from one position to the other. Separation of various components contained in the carrier gas is usually effected either by filling the sampling column with an appropriate chromatographic material, or with an additional chromatographic column connected in place of the restrictor. The latter can be accommodated in the same oven as the sampling column or in a separate oven and heated at a different temperature.

2.3.2.2. Theory. If pure carrier gas is passing through the sampling column, nothing happens on reversing the flow. But if a solute comes out of the diffusion column as the result of its diffusion into the carrier gas, filling the diffusion column and also running along the sampling column, the flow reversal records the concentration of the solute at the junction $x = l'$ (cf. Fig. 4) at the moment of the reversal. This concentration recording has the form of extra chromatographic peaks, we call *sample peaks* (cf. Fig. 5), superimposed on the otherwise continuous detector signal. The peak can be made as narrow as one wants, since the width at their half-height is equal to the duration of the backward flow of the carrier gas through the empty sampling column. The loading of the carrier gas with other substance(s) is due to its (their) slow diffusion into the carrier gas passing through the sampling column. The enrichment of carrier gas in the gas(es) contained in the diffusion column depends on the rate with which gas(es) enters (enter) the sampling column

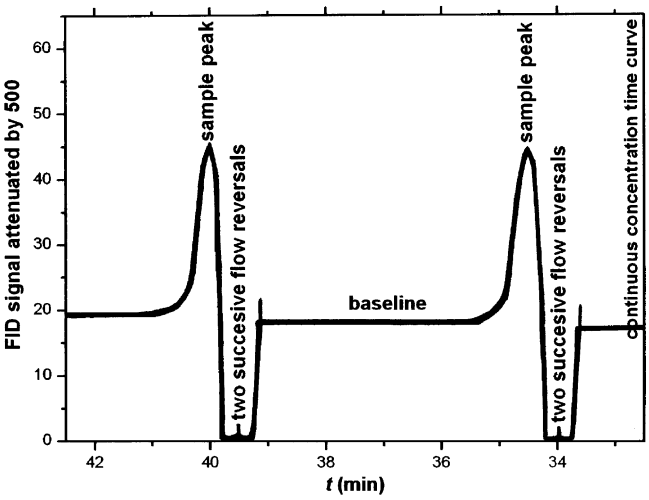

Fig. 5. A reversed-flow chromatogram showing two sample peaks for the diffusion of C_3H_6 into He ($\dot{V} = 0.283\,cm^3\,s^{-1}$) at 291 K and 1 atm.

at the junction $x = l'$ of the two columns. By reversing now the flow we perform a sampling of the concentration of the analyte gas at this junction, each sample peak measuring (by its height) this concentration at the time of the flow reversal. Repeating this sampling procedure at various times and using suitable mathematical analysis, the rate coefficient of the slow process responsible for the sample peaks can be determined, e.g. the diffusion coefficient of the analyte gas into the carrier gas.

The area under the curve or the height H from the continuous signal of the sample peaks, measured as a function of the time t when the flow reversal is made, is proportional to the concentration of the substance under study at the junction $x = l'$ of the sampling cell, at time t [50–58]:

$$H^{1/M} = gc(l', t) \tag{19}$$

where M is the response factor of the detector and g a proportionality constant pertaining to the detector calibration. Measuring H experimentally as a function of t, one can construct the *diffusion band*, the shape and the distortion of which leads to the determination of diffusion coefficient of gases in gases and liquids and on solids.

The concentration of the solute vapor in the diffusion column L, $c_z = c_z(z, t)$, is governed by the Fick's second law:

$$\frac{\partial c_z}{\partial t} = D_{AB} \cdot \frac{\partial^2 c_z}{\partial z^2} \tag{20}$$

which must be solved under the following initial and boundary conditions

$$c_z(z, 0) = \frac{m}{a} \cdot \delta(z - L) \tag{21}$$

$$c_z(0, t) = c(l', t), \quad \left(\frac{\partial c_z}{\partial t}\right)_{z=L} = 0 \tag{22}$$

$$D_{AB}\left(\frac{\partial c_z}{\partial z}\right)_{z=0} = \dot{v}c(l', t) \tag{23}$$

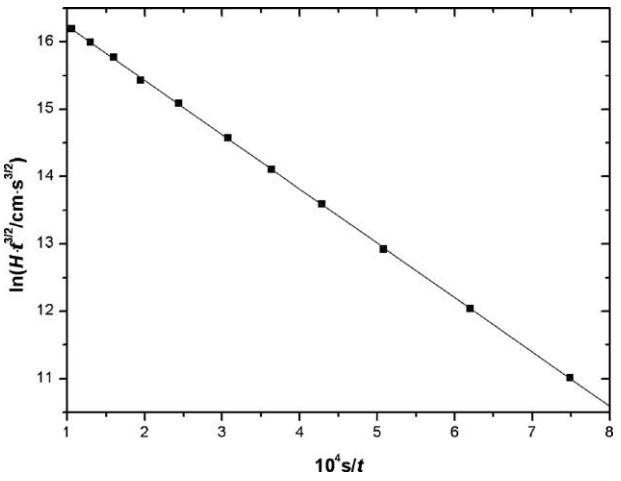

Fig. 6. Plot of Eq. (24) for the diffusion of C_2H_6 into N_2 at 388.5 K and 1 atm [58].

where m is the amount of solute injected, a is the cross-sectional area of void space in the column L, $\delta(z-L)$ is the Dirac delta function describing the mode of introducing the solute into column L through the point $z = L$, and υ is the linear velocity of the carrier gas.

Following suitable mathematical analysis presented previously [53–61], the following Equations describing the variation of H with t, when the slow process under study is the gaseous diffusion, are derived:

$$\ln(H^{1/M}t^{3/2}) = \log(gN_1) - \frac{L^2}{4D_{AB}} \cdot \frac{1}{t} \quad (24)$$

$$\ln(H^{1/M}) = \ln(gN_2) - \frac{3D_{AB}}{L^2} \cdot t \quad (25)$$

where

$$N_1 = \frac{mL}{\dot{V}(\pi D_{AB})^{1/2}} \quad (26)$$

$$N_2 = \frac{\pi m D_{AB}}{\dot{V}L^2} \quad (27)$$

where m is the injected amount of solute in mol and $\dot{V}$ is the volumetric flow-rate in $cm^3\,s^{-1}$.

Plotting the left-hand side of Eq. (24), $\ln(H^{1/M}t^{3/2})$ versus $1/t$, one can obtain the diffusion coefficient value of D_{AB} from the slope $-L^2/4D_{AB}$ of the straight line obtained and the known value of the diffusion column length (L).

Eq. (25) shows that a plot of $\ln H$ versus t (after the maximum of the diffusion band) is linear (cf. Fig. 6) with a slope $-3D_{AB}/L^2$, from which the diffusion coefficient D_{AB} can be also determined.

The question now naturally arising is: which one of the two equations, namely the Eqs. (24) and (25) is more accurate in the determination of the gaseous diffusion coefficients? The answer is not so simple and depends on both the gaseous system under study and the experimental conditions applied. Generally, Eq. (24) is used for short duration's experiments and for long diffusion columns, while Eq. (25) is used for short column lengths (say 30–50 cm) and for experiments of longer duration. The selection of the proper mathematical analysis to estimate the more accurate gaseous diffusion coefficient by RF-GC can be also based on the comparison of the two experimental values found from Eqs. (24) and (25) with those given in literature or calculated from known empirical equations.

The choice between Eqs. (24) and (25) is a matter also of preliminary experimentation with a gas of known D_{AB} value, possibly close to that expected for the unknown D_{AB}.

2.3.2.3. Results and discussion.

Diffusion coefficients in binary gas mixtures. The diffusion coefficients of various gaseous hydrocarbons in carrier gases N_2, H_2 and He determined by the reversed-flow technique with the aid of Eq. (24) at various temperatures are compiled in Tables 5–7.

The values and their standard errors found by regression analysis using standard least-squares procedures, are reduced to 1 atm after multiplication by the pressure of the experiment. This pressure is given in Table 5, so that one can find the actual values determined from the ratio D_{AB}/p. For the pair ethylene–nitrogen, the diffusion coefficient was determined at three different pressures, and for the pair methane–helium at two pressures. In both cases, the variation of the results with small changes in pressure (and in $\dot{V}$) is small.

The precision of the method, defined as the relative standard deviation (%), can be judged from the data given for methane–helium. From the five values quoted, a precision of 0.9% is calculated.

The experimental values of diffusion coefficient given in Table 5 are compared with those calculated theoretically by the Equation of HBS (Eq. (6)). Some literature values of the same diffusion coefficients are also given in the same table.

The calculated values in Table 5 are for the temperature of the experiment while the literature values refer to temperatures which differ from those of the present work by not more than 5 °C. The accuracy given in the last column of Table 5 is a measure of the deviation of the values found by the RF-GC method from the calculated ones, defined as:

$$\text{accuracy}\,(\%) = \frac{|D_{AB}^{found} - D_{AB}^{calcd}|}{D_{AB}^{found}} \times 100 \quad (28)$$

With the exception of two pairs containing methane as solute, this accuracy is better than 7.1% in all cases and in 8 out of the 15 pairs is better than 2.5%. The high deviation of the experimental from the calculated values for the pairs methane–nitrogen and methane–helium, in spite of the fact that the precision is 0.9% as mentioned before, is probably due to the approximations used in the calculated values. Finally, the accuracies of the present values can be compared with the accuracies of the respective literature values, given

Table 5
Diffusion coefficients of various solutes into three carrier gases at ambient temperatures and reduced to 1 atm pressure, determined by reversed-flow gas chromatography

Carrier gas	Solute gas	T (K)	$\dot{V}$ ($cm^3\,s^{-1}$)	p (atm)	D_{AB} ($\times 10^3\,cm^2\,s^{-1}$)			Accuracy[b] (%)
					Present work	Calculated	Literature [reference]	
N_2	CH_4	296.0	0.260	1.96	272 ± 4	214	–	21.3
	C_2H_6	293.0	0.267	1.99	142 ± 0.03	144	148 [62]	1.4 (2.7)
	n-C_4H_{10}	295.5	0.300	2.15	98 ± 0.2	98.6[a]	96 [62]	0.3 (2.7)
	C_2H_4	296.0	0.120	1.49	168 ± 2	156	163 [62]	7.1 (4.3)
		292.0	0.268	2.00	156 ± 0.4			0
		292.0	0.538	2.71	161 ± 0.4			3.1
	C_3H_6	298.0	0.260	1.96	124 ± 0.4	120[a]	–	3.2
H_2	CH_4	293.0	0.287	1.70	699 ± 3	705	730 [16]	0.9 (3.4)
	C_2H_6	297.0	0.267	1.56	548 ± 5	556	540 [16]	1.5 (3.0)
	n-C_4H_{10}	296.0	0.273	1.60	386 ± 3	373	400 [16]	3.4 (6.8)
	C_2H_4	293.0	0.300	1.75	525 ± 5	559	602 [62]	6.5 (7.1)
	C_3H_6	296.0	0.273	1.60	485 ± 3	486	–	0.2
He	CH_4	295.7	0.250	1.78	527 ± 3	669	–	26.9
		295.0	0.283	2.03	520 ± 1			28.7
		296.0	0.283	2.03	522 ± 1			28.2
		296.0	0.283	2.03	514 ± 0.2			30.2
		296.7	0.283	2.03	522 ± 3			28.2
	C_2H_6	295.6	0.300	2.15	518 ± 3	507	–	2.1
	n-C_4H_{10}	290.0	0.283	2.03	333 ± 3	330	364 [25]	0.9 (9.3)
	C_2H_4	296.0	0.283	2.03	558 ± 4	544	–	2.5
	C_3H_6	291.0	0.283	2.03	412 ± 4	440	–	6.8

The actual values found at the pressure of the experiment, p, are simply D_{AB}/p. All errors given in this and the following tables are "standard errors" calculated by regression analysis.

[a] The necessary parameters σ and ε/k were obtained from [2].

[b] This is defined by Eq. (33). Numbers in parentheses are the accuracies of the respective literature values.

Table 6
Diffusion coefficients of three solutes into carrier gas helium, at various temperatures and 1 atm pressure, determined by RF-GC

Solute gas	T (K)	D_{AB} ($\times 10^3\,cm^2\,s^{-1}$)		Accuracy (%)
		This work	Calculated	
C_2H_6	296.7	491 ± 2	456	7.1
	322.6	556 ± 2	528	5.0
	344.0	618 ± 3	590	4.5
	364.4	684 ± 3	653	4.5
	385.3	745 ± 6	720	3.4
	407.3	807 ± 4	793	1.7
	426.3	878 ± 8	859	2.2
	447.3	941 ± 5	935	0.6
C_2H_4	296.8	525 ± 4	478	9.0
	322.9	599 ± 1	554	7.5
	336.0	649 ± 1	594	8.5
	348.1	674 ± 2	632	6.2
	361.3	726 ± 2	674	7.2
	373.9	780 ± 6	716	8.2
	399.9	860 ± 19	806	6.3
	426.9	932 ± 3	903	3.1
	476.5	1112 ± 10	1096	1.4
C_3H_6	345.0	528 ± 0.7	500	5.3
	365.5	584 ± 1	533	5.3
	388.0	642 ± 1	614	4.4
	407.7	690 ± 1	670	2.9
	428.0	750 ± 2	730	2.7
	449.4	819 ± 3	795	2.9

Table 7
Diffusion coefficients of three solutes into carrier gas nitrogen, at various temperatures and 1 atm pressure, determined by RF-GC

Solute gas	T (K)	D_{AB} ($\times 10^3\,cm^2\,s^{-1}$)		Accuracy (%)
		This work	Calculated	
C_2H_6	322.8	172 ± 0.2	170	1.2
	345.7	193 ± 0.2	191	1.0
	365.0	214 ± 0.7	210	1.9
	388.5	242 ± 0.3	234	3.3
	407.6	256 ± 0.2	255	0.4
	427.5	282 ± 0.4	277	1.8
	449.3	303 ± 0.5	302	0.3
C_2H_4	322.8	189 ± 0.08	179	5.3
	344.7	213 ± 0.1	200	6.1
	364.2	234 ± 0.3	221	5.6
	387.6	260 ± 0.3	246	5.4
	407.5	286 ± 0.4	269	5.9
	428.9	306 ± 0.3	294	3.9
	449.8	335 ± 0.9	319	4.8
C_3H_6	322.8	143 ± 0.2	138	3.5
	344.6	164 ± 0.1	155	5.5
	387.4	20 ± 0.2	190	5.9
	406.4	220 ± 0.4	206	6.4
	428.9	243 ± 0.3	227	6.6
	459.0	266 ± 0.2	255	4.1

in parentheses in Table 5 and defined again by Eq. (28) with D_{AB}^{lit} in place of D_{AB}^{found}. This comparison leads to the conclusion that, with the exception of ethylene–nitrogen, the values of diffusion coefficients determined by the RF-GC method are closer to the theoretical calculated values than are the experimental values found in the literature, under similar conditions of temperature and pressure.

One final remark is that the D_{AB} values determined by the reversed-flow method are very sensitive to the precision with which L is measured, since D_{AB} is proportional to L^2. Instead of measuring directly the length L, one can use a solute–carrier gas pair of accurately known diffusion coefficient, and carry out a calibration experiment for L. The value of L so calculated can now be used to estimate unknown diffusion coefficients.

In conclusion, with the aid of simple GC instrumentation, precise and accurate mutual diffusion coefficients in gases can be determined. The method has certain instrumental similarities with a technique reported by Desty et al. [63]. They used the diffusion of vapor from a liquid surface through a stagnant column of gas in a capillary tube, to maintain constant low concentrations of the vapor in a gas stream, in order to study the performance of a flame-ionization detector. They also described how to determine the rate of diffusion from the open end of the capillary by measuring the distance between this end and the liquid meniscus as a function of time.

The theoretical values of diffusion coefficients in Tables 6 and 7 were computed using the FSG equation (Eq. (7)). The FSG equation for the estimation of the theoretical diffusion coefficients [4] was selected because it gives values closer to those found experimentally than other theoretical equations. Thus, the average accuracy for the 43 diffusion coefficients listed in Tables 6 and 7 is 4.4%, whereas it would be 7.3% if, instead of FSG, the HBS equation (Eq. (5)) was used.

All of the theoretical or semi-empirical equations describing the dependence of the diffusion coefficient on temperature lead to the relationship:

$$D_{AB} = AT^n \quad (29)$$

where A is a complex function including molar masses or volumes, critical volumes or temperatures, volume increments, pressure, etc., depending on the special equation used. Eq. (29) shows that the exponent n can be found from the slopes of the linear plots of $\ln D_{AB}$ against $\ln T$. An example of such a plot, using experimental data from this work, is shown in Fig. 7. The various values of n calculated from these plots, denoted as n_{found}, are given in Table 8. For comparison purposes, the values of n found from similar plots of calculated diffusion coefficients (using the HBS equation) are also given. The use of this equation is due to the reason that is the only one in which the exponent n varies from one system to another. The mean values of n_{found} listed in Table 8 are somewhere between the 1.5 suggested by the Stefan–Maxwell, Gilliland and Arnold equation [1,64,65] and 1.81 predicted by the Chen–Othmer (CO) equation [1].

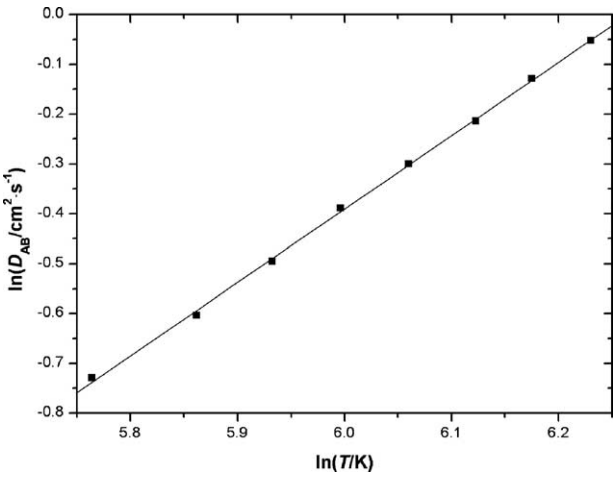

Fig. 7. Plot of Eq. (29) for the diffusion of C_2H_6 into He ($p = 1$ atm) [58].

A value of 1.75 is also predicted by the Huang [3] and the FSG equations.

Seager et al. [19] investigated experimentally (with a different method) the temperature dependence of gas–gas and gas–liquid vapor diffusion coefficients. They found that the value of exponent n varied rather widely from one system to another. Their average value of n (1.70) was very close to the experimental values determined by RF-GC. Hargrove and Sawyer [25] determined the diffusion coefficients for a variety of solutes at various temperatures and found a value of n varying from 1.43 to 1.93, depending on the binary system studied. The RF-GC mean values of n again lie within this range.

As a general conclusion, one can say that the RF-GC method for measuring mutual diffusion coefficients in gases gives fairly accurate values of diffusion coefficients at relatively high temperatures. It is therefore suitable for studying the temperature variation of gas diffusion coefficients.

Diffusion coefficients of binary mixtures into pure gases. The reversed-flow method for measurement of gas diffusion coefficients in binary mixtures, presented previously, was also extended to simultaneous determination of effec-

Table 8
Values of the exponent n of Eq. (29) calculated from the present experimental data (n_{found}) and from theoretical diffusion coefficients (calculated from Hirschfelder–Bird–Spotz equation) (n_{calcd})

Carier gas	Solute gas	n_{found}	n_{calcd}
He	C_2H_6	1.60 ± 0.01	1.680 ± 0.002
	C_2H_4	1.59 ± 0.03	1.671 ± 0.002
	C_3H_6	1.63 ± 0.02	1.685 ± 0.003
Mean value		1.61 ± 0.01	1.679 ± 0.001
N_2	C_2H_6	1.73 ± 0.04	1.801 ± 0.008
	C_2H_4	1.71 ± 0.02	1.779 ± 0.005
	C_3H_6	1.77 ± 0.05	1.844 ± 0.008
Mean value		1.74 ± 0.02	1.808 ± 0.004

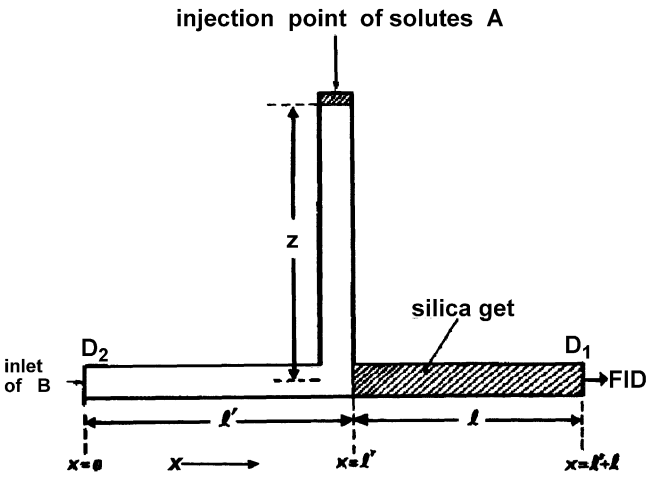

Fig. 8. Schematic representation of cell used to measure diffusion coefficients in multicomponent gas mixtures by RF-GC [66].

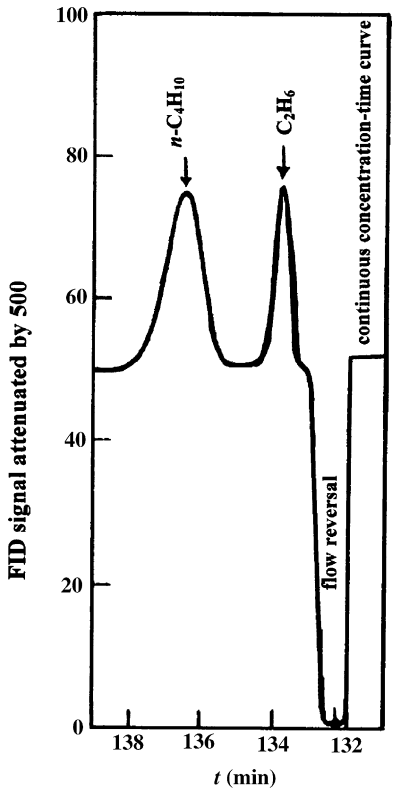

Fig. 9. Reversed-flow chromatogram for simultaneous determination of diffusion coefficients in ternary mixture of two solutes ($C_2H_6 + n$-C_4H_{10}) and carrier gas H_2. $T = 292$ K, $p = 1.7$ atm [66].

tive diffusion coefficients for each substance in a multicomponent gas mixture [66]. This extension of the method is achieved by filling the column section l (cf. Fig. 8) with a chromatographic material, which can effect the separation of all components of the gas mixture. When the "chromatographic sampling" is then performed, by reversing the direction of the gas flow for a short time (10–30 s) and restoring it to its original direction after that, two or more (depending on the components of the mixture injected) extra symmetrical peaks appear in the chromatogram (cf. Fig. 9). For each of these components Eq. (24) holds true, the only difference being the pairs of the experimental parameters H ant t, measured by RF-GC. Therefore a separate plot of $\ln(Ht^{3/2})$ against $1/t$ for each component yields its effective binary diffusion coefficient of the diffusion of it in the mixture from the slope $-L^2/4D_{AB}$ (cf. Fig. 10).

The effective diffusion coefficients of various mixtures of gaseous hydrocarbons (1:1, w/w) into the carrier gases N_2, H_2 and He, D_1 and D_2, determined by RF-GC, with the aid of Eq. (24), are listed in Table 9. In the same table are compiled calculated theoretical values [3] for the diffusion of each hydrocarbon in pure carrier gas. A comparison between the experimental and the calculated values from the HBS equation (Eq. (6)) shows a percentage difference ranging from 0.3 to 7.9%, with one exception (n-C_4H_{10} in N_2), being in that case 16%. These differences are of about the same magnitude as the percentage accuracy (0.3–7.1%) found experimentally for the diffusion of the same hydrocarbons in the corresponding pure carrier gases [56]. This is in accord with a limiting case of the Stefan–Maxwell equations [3] which predict that, for small mole fractions of components 1 and 2 in nearly pure carrier gas, the effective diffusion coefficient in the ternary mixture is equal to the diffusion coefficient of each component in pure carrier gas. The presence of the chromatographic material (silica gel) in column

Table 9
Effective diffusion coefficients reduced to 1 atm in some ternary mixtures comprising carrier gas and two hydrocarbons

Carrier gas	Solute gases		T (K)	D_{AB} ($\times 10^3$ cm^2 s^{-1})		D_{AB} ($\times 10^3$ cm^2 s^{-1})	
	1	2		Experimental	Calculated	Experimental	Calculated
H_2	C_2H_4	C_2H_6	298	554 ± 15	593	600 ±7	557
	C_2H_4	n-C_4H_{10}	296	586 ± 37	584	381 ± 13	379
	C_2H_6	n-C_4H_{10}	292	534 ± 9	538	379 ± 8	372
	C_2H_6	n-C_4H_{10}	292	503 ± 17	538	360 ± 14	372
	C_2H_6	–	297	556 ± 13	556	–	–
He	C_2H_6	n-C_4H_{10}	294	494 ± 7	506	354 ± 7	338
N_2	C_2H_4	n-C_4H_{10}	296	166 ± 4	156	118 ± 3	99

Experimental values are effective diffusion coefficients in ternary mixtures, while calculated ones refer to diffusion in pure carrier gas.

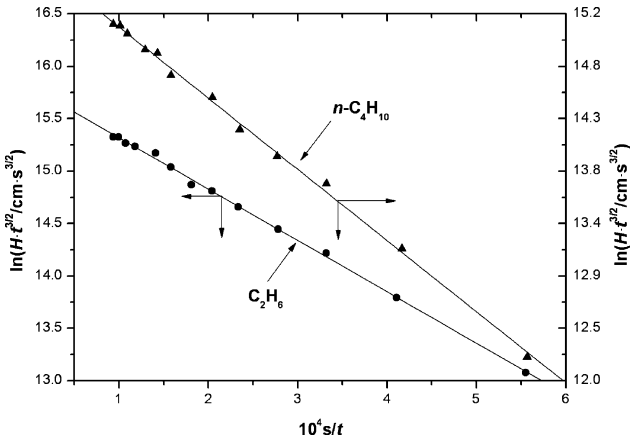

Fig. 10. Plot of Eq. (24) for the diffusion of $C_2H_6 + n$-C_4H_{10} into He at 294 K and 2.2 atm [66].

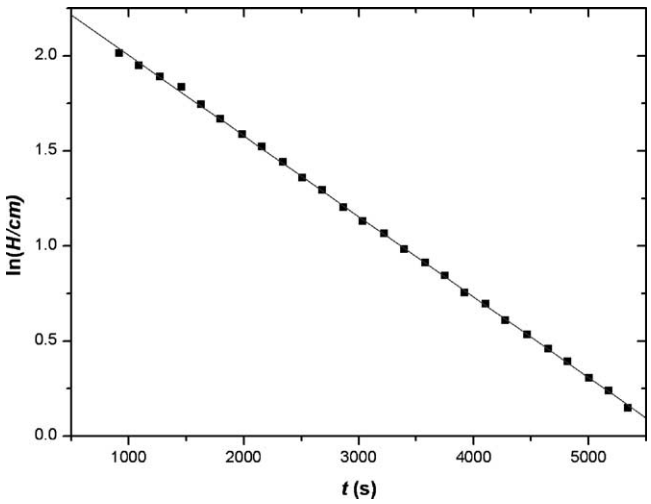

Fig. 11. Plot of Eq. (25) for the diffusion of CO_2 into the mixture 49.95% H_2 + 50.05% He at 324.7 K and 1 atm [60].

l does not seem to influence the values of the diffusion coefficients found. An additional indication of this is given in Table 9, where a binary mixture ($H_2 + C_2H_6$) is included. The diffusion coefficient found not only coincides with the theoretical calculated value, but also is not significantly different from the value 0.548 $cm^2\,s^{-1}$ found in previous work [56] with the empty column l.

Diffusion coefficients of pure gases into gas mixtures. The reversed-flow technique was also applied for the measurement of diffusion coefficients of pure gases into gas mixtures [59,60]. The details of the experimental setup have been described previously for the determination of the diffusion coefficients of pure gases and binary gas mixtures into pure carrier gases, the only difference being that the carrier gases were mixtures of H_2 and He with various percentage volume compositions (25.05% H_2 + 74.95% He, 49.95% H_2 + 50.05% He, and 75.05% H_2 + 24.95% He). The analyte gases used were CO and CO_2. The diffusion (L) and sampling columns (l and l'), which are empty of any chromatographic material, are placed inside the chromatographic oven. At a given time after injecting 1 ml of the analyte gas (CO or CO_2) into the diffusion column, during which no signal is noted, an asymmetrical concentration–time curve for the gas is recorded (rising slowly and decaying more slowly). During the whole experimental period, flow reversals for a time period of 6 s, which is smaller than both the gas hold times in columns l and l' are carried out by a four-port valve. This give rise to a series of peaks like those of Fig. 5 corresponding with various times from the solute injection. The plot of $\ln H$ versus t (after maximum) is linear, during the whole experiment, according to Eq. (25) (cf. Fig. 11), thus making possible the determination of the diffusion coefficient of the pure gases CO and CO_2 into the mixtures of H_2 and He from the slope $-3D_{AB}/L^2$ of the linear part of Fig. 11 (Tables 10 and 11).

The linear regression analysis of D_{mix}^{exp} for CO and CO_2 into various mixtures of H_2 and He against the hydrogen percentage volume composition (X_{H_2}) at all temperatures referred to in Tables 10 and 11 resulted in the following empirical equation relating D_{mix}^{exp} to the individual diffusion coefficients of CO and CO_2 into the pure H_2 (D_{H_2}) and He (D_{He}), as they are calculated from the FSG equation [18], as well as to the given percentage volume composition of the gas mixture [59,60]:

$$D_{mix} = X_{H_2} D_{H_2} + X_{He} D_{He} \quad (30)$$

In order to test the validity of Eq. (30), because the diffusion coefficient is not generally an additive parameter, one can calculate the diffusion coefficients of CO and CO_2 into the various gas mixtures with the known volume composition at all of the working temperatures, D_{mix}^{cal}, using as D_{H_2} and D_{He} values those calculated from the FSG equation (Tables 10 and 11). The accuracy given in the last column of Tables 10 and 11 is a measure of the deviation of the experimental values of RF-GC, D_{mix}^{exp} from the calculated ones, D_{mix}^{cal}, which is defined as:

$$\text{accuracy}\,(\%) = \frac{|D_{mix}^{exp} - D_{mix}^{cal}|}{D_{mix}^{exp}} \times 100 \quad (31)$$

In all cases, the accuracy is very good because the percentage deviation is lower than 0.66 indicating that the empirical Eq. (30) is valid at least for the systems used and the gas volume compositions applied.

The choice of the FSG equation to calculate the D_{H_2} and D_{He} values that are to be used in Eq. (30) for the estimation of the D_{mix}^{exp} is based on the fact the D_{mix}^{exp} is closer to D_{mix}^{cal} based on the FSG equation. For comparison purposes, except for the FSG equation, the SM, HBS, and CO equations [4,19,21] are also used (cf. Tables 12 and 13). The average percentage deviation of the D_{mix}^{exp} calculated from Eq. (30) using as D_{H_2} and D_{He} the values estimated from the FSG, SM, HBS, and CO equations are 0.18, 19.22,

Table 10
Experimental, D_{mix}^{exp}, and theoretical, D_{mix}^{cal}, as calculated from Eq. (30), diffusion coefficients of CO into mixtures of H_2 and He of various volume composition of hydrogen, X_{H_2}, at various temperatures[a]

T (K)	X_{H_2} (%)	D_{mix}^{exp} ($cm^2\ s^{-1}$)	D_{mix}^{cal} ($cm^2\ s^{-1}$)	Accuracy[b] (%)
315.2	0	0.754	0.754	0.00
	25.05	0.771	0.770	0.13
	49.95	0.788	0.787	0.13
	75.05	0.804	0.803	0.12
	100	0.820	0.819	0.12
320.0	0	0.775	0.775	0.00
	25.05	0.789	0.791	0.25
	49.95	0.806	0.808	0.25
	75.05	0.826	0.824	0.24
	100	0.842	0.840	0.24
324.7	0	0.796	0.795	0.13
	25.05	0.813	0.812	0.12
	49.95	0.829	0.829	0.00
	75.05	0.847	0.845	0.24
	100	0.863	0.862	0.12
329.4	0	0.818	0.815	0.37
	25.05	0.834	0.832	0.24
	49.95	0.851	0.850	0.12
	75.05	0.868	0.867	0.12
	100	0.883	0.884	0.11
334.2	0	0.836	0.836	0.00
	25.05	0.851	0.854	0.35
	49.95	0.869	0.872	0.35
	75.05	0.891	0.889	0.22
	100	0.903	0.907	0.44
339.0	0	0.859	0.857	0.23
	25.05	0.876	0.875	0.11
	49.95	0.895	0.894	0.11
	75.05	0.913	0.912	0.11
	100	0.931	0.930	0.11
343.9	0	0.882	0.879	0.34
	25.05	0.899	0.897	0.22
	49.95	0.918	0.913	0.22
	75.05	0.937	0.934	0.32
	100	0.954	0.953	0.10

[a] $p = 1$ atm.
[b] Defined by Eq. (31).

Table 11
Experimental, D_{mix}^{exp}, and theoretical, D_{mix}^{cal}, as calculated from Eq. (30), diffusion coefficients of CO_2 into mixtures of H_2 and He of various volume composition of hydrogen, X_{H_2}, at various temperatures[a]

T (K)	X_{H_2} (%)	D_{mix}^{exp} ($cm^2\ s^{-1}$)	D_{mix}^{cal} ($cm^2\ s^{-1}$)	Accuracy[b] (%)
315.2	0	0.511	0.509	0.39
	25.05	0.555	0.558	0.54
	49.95	0.608	0.606	0.33
	75.05	0.656	0.655	0.15
	100	0.700	0.703	0.43
320.0	0	0.526	0.523	0.57
	25.05	0.570	0.573	0.52
	49.95	0.624	0.622	0.32
	75.05	0.670	0.672	0.30
	100	0.724	0.722	0.28
324.7	0	0.534	0.537	0.56
	25.05	0.589	0.588	0.17
	49.95	0.636	0.638	0.31
	75.05	0.691	0.689	0.29
	100	0.738	0.740	0.27
329.4	0	0.552	0.550	0.36
	25.05	0.599	0.603	0.66
	49.95	0.657	0.655	0.31
	75.05	0.704	0.808	0.56
	100	0.761	0.760	0.13
334.2	0	0.566	0.564	0.35
	25.05	0.615	0.618	0.49
	49.95	0.673	0.672	0.15
	75.05	0.727	0.725	0.28
	100	0.782	0.779	0.39
339.0	0	0.580	0.579	0.17
	25.05	0.635	0.634	0.16
	49.95	0.690	0.688	0.29
	75.05	0.745	0.743	0.27
	100	0.796	0.798	0.25
343.9	0	0.596	0.593	0.51
	25.05	0.647	0.650	0.46
	49.95	0.709	0.706	0.42
	75.05	0.759	0.763	0.52
	100	0.820	0.819	0.12

[a] $p = 1$ atm.
[b] Defined by Eq. (31).

9.07, and 8.37%, respectively, for CO, and 0.35, 7.40, 9.83, and 23.95%, respectively, for CO_2. These results indicate that the FSG equation has the higher accuracy of all of the tested empirical equations, because this relationship is the result of the fitting of more than 340 experimental diffusion coefficients owing to 153 different binary mixtures [1,4].

2.4. Sources of errors

Several problems are associated with gaseous diffusion-coefficient measurements [9].

The main problem of the continuous elution method is that of extra zone broadening factors, also mentioned in the experimental part. The use of two columns initially suggested by Giddings and Seager [17] is absolutely necessary when any significant amount of dead volume is present.

Ideally, the sample would enter the column as an infinitely narrow plug something difficult to approach experimentally. Ingenious injection devices [15] can be used. The basic design is such that the sample gas or vapor flows continuously through one part of the device and the carrier gas flows through another. At the moment of injection a portion of the sample is trapped and then placed in the carrier gas stream.

Careful attention must be paid to ensuring that temperature gradients are kept to a minimum in a vicinity of the column. This problem can be eliminated through careful

Table 12
Experimental, D_{mix}^{exp}, and theoretical, D_{mix}^{cal}, as calculated from Eq. (30), diffusion coefficients of CO into mixtures of H_2 and He of various volume composition of H_2, X_{H_2}, at various temperatures[a], using various empirical equations for the estimation of the diffusion coefficient of CO into pure H_2 and He

T (K)	X_{H_2} (%)	D_{mix}^{exp} ($cm^2\,s^{-1}$)	D_{mix}^{cal} ($cm^2\,s^{-1}$)				Deviation[b] (%)			
			FSG	SM	HBS	CO	FSG	SM	HBS	CO
315.2	0	0.754	0.754	0.578	0.718	0.847	0.00	23.34	4.77	12.33
	25.05	0.771	0.770	0.611	0.715	0.848	0.13	20.75	7.26	9.99
	49.95	0.788	0.787	0.644	0.712	0.850	0.13	18.27	9.64	7.87
	75.05	0.804	0.803	0.676	0.709	0.852	0.12	15.92	11.82	5.97
	100	0.820	0.819	0.709	0.706	0.854	0.12	13.54	13.90	4.15
320.0	0	0.775	0.775	0.592	0.739	0.870	0.00	23.61	4.65	12.26
	25.05	0.789	0.791	0.625	0.736	0.872	0.25	20.79	6.72	10.52
	49.95	0.806	0.808	0.659	0.732	0.874	0.25	18.24	9.18	8.44
	75.05	0.826	0.824	0.692	0.729	0.876	0.24	16.22	11.74	6.05
	100	0.842	0.840	0.725	0.726	0.878	0.24	13.90	13.78	4.28
324.7	0	0.796	0.795	0.605	0.760	0.893	0.13	23.99	4.52	12.19
	25.05	0.813	0.812	0.639	0.756	0.895	0.12	21.40	7.01	10.09
	49.95	0.829	0.829	0.673	0.752	0.897	0.00	18.82	9.29	8.20
	75.05	0.847	0.845	0.707	0.748	0.899	0.24	16.53	11.69	6.14
	100	0.863	0.862	0.741	0.745	0.901	0.12	14.14	13.67	4.40
329.4	0	0.818	0.815	0.618	0.781	0.917	0.37	24.45	4.52	12.10
	25.05	0.834	0.832	0.653	0.776	0.919	0.24	21.70	6.95	10.19
	49.95	0.851	0.850	0.688	0.772	0.921	0.12	19.15	9.28	8.23
	75.05	0.868	0.867	0.723	0.768	0.923	0.12	16.71	11.52	6.34
	100	0.883	0.884	0.758	0.764	0.925	0.11	14.16	13.48	4.76
334.2	0	0.836	0.836	0.631	0.802	0.941	0.00	24.52	4.07	12.56
	25.05	0.851	0.854	0.667	0.798	0.943	0.35	21.62	6.23	10.81
	49.95	0.869	0.872	0.703	0.793	0.945	0.35	19.10	8.75	8.75
	75.05	0.891	0.889	0.739	0.789	0.947	0.22	17.06	11.45	6.29
	100	0.903	0.907	0.774	0.784	0.949	0.44	14.29	13.18	5.09
339.0	0	0.859	0.857	0.645	0.824	0.966	0.23	24.91	4.07	12.46
	25.05	0.876	0.875	0.682	0.819	0.968	0.11	22.15	6.51	10.50
	49.95	0.895	0.894	0.718	0.815	0.970	0.11	19.78	8.94	8.38
	75.05	0.913	0.912	0.755	0.810	0.972	0.11	17.31	11.28	6.46
	100	0.931	0.930	0.791	0.805	0.974	0.11	15.04	13.53	4.62
343.9	0	0.882	0.879	0.659	0.847	0.991	0.34	25.28	3.97	12.36
	25.05	0.899	0.897	0.694	0.842	0.993	0.22	22.80	6.34	10.46
	49.95	0.918	0.913	0.734	0.836	0.996	0.22	20.04	8.93	8.50
	75.05	0.937	0.934	0.771	0.831	0.998	0.32	17.72	11.31	6.51
	100	0.954	0.953	0.808	0.826	1.000	0.10	15.30	13.42	4.82
Mean value of deviation (%)							0.18	19.22	9.07	8.37

[a] $p = 1$ atm.

[b] Deviation (%) $= \dfrac{|D_{mix}^{exp} - D_{mix}^{cal}|}{D_{mix}^{exp}} \times 100.$

arrangement of the oven geometry [36], or using a liquid constant temperature bath [28].

It is also important to ensuring a steady flow of the carrier gas. Carrier gas flow irregularities are most apt to be a problem when injection valves are used, since the steady flow of carrier gas is interrupted at the moment of injection. However, such valves are desirable because injection volume is far more reproducible and the injection profile approximates a δ function.

Other sources of errors are due to secondary flow, race-track effect, and stagnant pockets. Careful instrumentation design (e.g. large coil diameter, slow flow-rates, and minimum dead volumes) can greatly diminish these difficulties [5].

The concentration effect on D_{AB}, the linearity of the electronics, and the buoyant effect need to be carefully estimated and chosen. The above factors which may affect the zone dispersion or the shape of the peak in all forms of GC system can be neglected when a small enough sample is employed [37].

Solute's adsorption on the column wall can also contribute to the peak width. Therefore, tubes containing low-energy adsorption sites and small ratios of wall surface to volume should be used.

Table 13
Experimental, D_{mix}^{exp}, and theoretical, D_{mix}^{cal}, as calculated from Eq. (30), diffusion coefficients of CO_2 into mixtures of H_2 and He of various volume composition of H_2, X_{H_2}, at various temperatures[a], using various empirical equations for the estimation of the diffusion coefficient of CO_2 into pure H_2 and He

T (K)	X_{H_2} (%)	D_{mix}^{exp} ($cm^2\,s^{-1}$)	D_{mix}^{cal} ($cm^2\,s^{-1}$)				Deviation[b] (%)			
			FSG	SM	HBS	CO	FSG	SM	HBS	CO
315.2	0	0.511	0.509	0.503	0.559	0.733	0.39	1.57	9.39	43.44
	25.05	0.555	0.558	0.534	0.562	0.737	0.54	3.78	1.26	32.79
	49.95	0.608	0.606	0.565	0.566	0.741	0.33	7.07	6.91	21.88
	75.05	0.656	0.655	0.597	0.570	0.744	0.15	8.99	13.11	13.41
	100	0.700	0.703	0.628	0.573	0.748	0.43	10.29	18.14	6.86
320.0	0	0.526	0.523	0.515	0.575	0.754	0.57	2.09	9.32	43.35
	25.05	0.570	0.573	0.547	0.578	0.757	0.52	4.04	1.40	32.81
	49.95	0.624	0.622	0.578	0.582	0.761	0.32	7.37	6.73	21.96
	75.05	0.670	0.672	0.610	0.585	0.765	0.30	8.96	12.69	14.18
	100	0.724	0.722	0.642	0.588	0.768	0.28	11.33	18.78	6.08
324.7	0	0.534	0.537	0.526	0.590	0.774	0.56	1.50	10.49	44.94
	25.05	0.589	0.588	0.559	0.594	0.778	0.17	5.09	0.85	32.09
	49.95	0.636	0.638	0.591	0.597	0.781	0.31	7.08	6.13	22.80
	75.05	0.691	0.689	0.624	0.601	0.785	0.29	9.70	13.02	13.60
	100	0.738	0.740	0.656	0.604	0.789	0.27	11.11	18.16	6.91
329.4	0	0.552	0.550	0.538	0.606	0.794	0.36	2.54	9.78	43.84
	25.05	0.599	0.603	0.571	0.610	0.798	0.66	4.67	1.84	33.22
	49.95	0.657	0.655	0.604	0.613	0.802	0.31	8.07	6.70	22.07
	75.05	0.704	0.808	0.637	0.616	0.806	0.56	9.52	12.50	14.49
	100	0.761	0.760	0.671	0.620	0.810	0.13	11.83	18.53	6.44
334.2	0	0.566	0.564	0.549	0.623	0.815	0.35	3.00	10.07	43.99
	25.05	0.615	0.618	0.583	0.626	0.819	0.49	5.20	1.79	33.17
	49.95	0.673	0.672	0.617	0.629	0.823	0.15	8.32	6.54	22.29
	75.05	0.727	0.725	0.651	0.32	0.827	0.28	10.45	13.07	13.76
	100	0.782	0.779	0685	0.636	0.831	0.39	12.40	18.67	6.27
339.0	0	0.580	0.579	0.561	0.639	0.837	0.17	3.28	10.17	44.31
	25.05	0.635	0.634	0.596	0.642	0.841	0.16	6.14	1.10	33.44
	49.95	0.690	0.688	0.631	0.646	0.845	0.29	8.55	6.38	22.46
	75.05	0.745	0.743	0.665	0.649	0.849	0.27	10.74	12.89	13.96
	100	0.796	0.798	0.700	0.652	0.853	0.25	12.06	18.09	7.16
343.9	0	0.596	0.593	0.573	0.657	0.859	0.51	3.86	10.23	44.13
	25.05	0.647	0.650	0.609	0.660	0.863	0.46	5.87	2.01	33.38
	49.95	0.709	0.706	0.644	0.663	0.867	0.42	9.17	6.49	22.28
	75.05	0.759	0.763	0.680	0.666	0.871	0.52	10.41	12.25	14.76
	100	0.820	0.819	0.715	0.669	0.876	0.12	12.80	18.41	6.83
Mean value of deviation (%)							0.35	7.40	9.83	23.95

[a] $p = 1$ atm.

[b] Deviation (%) $= \dfrac{|D_{mix}^{exp} - D_{mix}^{cal}|}{D_{mix}^{exp}} \times 100.$

2.5. Comparison of the broadening with the flow perturbation techniques

2.5.1. Accuracy

The accuracy of the RF-GC technique for measuring gaseous diffusion coefficients, is compared with that of GC-BT by investigating the mean percentage deviation of their values D_{AB}^{RF} and D_{AB}^{BT} from the respective predicted D_{AB}^{cal} values by means of FSG equation. The mean percentage deviation of RF-GC is estimated 3.4, while that of the GC-BT, for the two binary gas mixtures presented in Table 14, for which consistent literature values are available, is 5.7. Consequently, the accuracy of RF-GC in comparison with the GC-BT is higher, at least for the studied gas mixtures.

2.5.2. Precision

The precision of the RF-GC method was judged from the data given in Table 5. From the values quoted a precision 0.9% was calculated. The precision of continuous elution GC-BT [17] was about 1%, while that of the arrested-elution GC-BT [20] was about 2%.

2.5.3. Experimental arrangement

The basic setup used by continuous elution GC-BT is a commercial GC apparatus where the packed column is

Table 14
Experimental diffusion coefficients from RF-GC (D_{AB}^{exp}) and literature values determined from GC broadening techniques (D_{AB}^{lit}) compared to theoretical ones (D_{AB}^{cal}) estimated by the FSG equation

Binary gas system	T (K)	D_{AB}^{exp} ($cm^2\,s^{-1}$)	D_{AB}^{cal} ($cm^2\,s^{-1}$)	D_{AB}^{lit} ($cm^2\,s^{-1}$)	Accuracy[a] (%)	Accuracy[b] (%)	Reference
C_2H_4–N_2	322.8	0.189	0.179	0.190	5.3	6.1	[24]
	344.7	0.213	0.200	0.214	6.1	7.0	[24]
	364.2	0.234	0.221	0.235	5.6	6.3	[24]
	387.6	0.260	0.246	0.262	5.4	6.5	[24]
	407.5	0.286	0.269	0.286	5.9	6.3	[24]
	428.9	0.306	0.294	0.313	3.9	6.5	[24]
	449.8	0.335	0.319	0.340	4.8	6.6	[24]
C_2H_6–N_2	322.8	0.172	0.170	0.161	1.2	5.3	[16]
	345.7	0.193	0.191	0.182	1.0	4.7	[16]
	365.0	0.214	0.210	0.200	1.9	4.8	[16]
	388.5	0.242	0.234	0.223	3.3	4.7	[16]
	407.6	0.256	0.255	0.242	0.4	5.1	[16]
	427.5	0.282	0.277	0.263	1.8	5.0	[16]
	449.3	0.303	0.302	0.287	0.3	5.0	[16]
Mean accuracy (%)					3.4	5.7	

[a] Accuracy (%) $= 100 \times \dfrac{|D_{AB}^{exp} - D_{AB}^{cal}|}{D_{AB}^{exp}}$.

[b] Accuracy (%) $= 100 \times \dfrac{|D_{AB}^{lit} - D_{AB}^{cal}|}{D_{AB}^{lit}}$.

replaced with a coiled, long, empty tube of circular cross-section. In the case of arrested elution broadening technique, however, packed columns have been used.

A similar but simpler, setup is used also by RF-GC. Its main advantage is the length of the empty diffusion column (cf. Fig. 4) being 30–80 cm, while in the case of continuous elution GC-BT much longer (∼15 m) columns have been used [11].

2.5.4. Experimental procedure

The time analysis for the determination of D_{AB} values for the continuous elution method is very short (≈5 min). Giddings and Seager [17] made 200 separate determinations in 36 h. In contrast, in the arrested elution GC-BT the time needed for a D_{AB} determination is longer (≈3 h), due to the requirement of repeating the experiment at a variety of delay times (1–20 min).

The time needed for the determination of D_{AB} values by RF-GC lies between those required by continuous elution and arrested elution broadening techniques. This time is about 30–60 min depending on the binary gas mixture and the length of the diffusion column used. Further shortening of the diffusion column and validation of the short time analysis method could decrease drastically the time needed for such a determination by RF-GC. In addition, the experimental setup of RF-GC permits the measurement of diffusion coefficient values in multicomponent gas mixtures [59,60,66].

2.5.5. Sources of errors

In continuous elution method extra zone broadening factors, such as secondary flow are also contribute to peak broadening. In order to eliminate the effect of any significant amount of dead volume, the use of two columns (see Section 2.2.3) is necessary.

The main advantage of the arrested elution broadening technique is that such a correction procedure is not necessary, resulting in more reliable D_{AB} values through a more time consuming procedure.

RF-GC being a dynamic technique under steady-state conditions has also the advantage that the extra zone broadening factors affecting the measurements in continuous elution broadening technique are not imply in D_{AB} determinations.

3. Diffusion of gases in liquids

Diffusion coefficients in liquids are increasingly important in many theoretical and engineering calculations involving mass transfer, such as absorption, extraction, distillation and chemical reactions. A big number of separation techniques, pollution problems and chemical reactions depend to a large extent on diffusing species in liquid media. For example, in the case of considering polymers as materials for industrial applications, the ability of small molecules diffusing through a polymeric phase, described by the diffusion coefficient, is of great importance. Moreover, the ingress of chemicals into storage tanks and pipes in the chemical and petroleum industries and the transfer of substances from container walls to packaged products in the food industry are also examples of applications where diffusion coefficients for small molecules at infinite dilution are needed.

In general, the measurement of accurate diffusion coefficients of gases in liquids is not an easy task. Different values are often obtained from different workers in different

laboratories even by using similar measuring techniques. Furthermore, close agreement between experimental values and theoretically predicted ones is not easily achieved.

Most methods used till seventies for the measurement of diffusion coefficients in liquid systems were based on static bulk equilibration methods (gravimetric sorption/desorption). However, static methods relied on sorption and bulk equilibration suffer from a serious limitation. There is difficulty to apply these techniques to solute–solvent systems where the solute is present in vanishingly small amounts, which is a demand of big importance frequently required for the design of many polymer synthesis and fabrication operations. As result the time for sorption may be large because the diffusion coefficient may be small. In addition accuracy suffers because the amount of solute is small.

In the early 1950s, Taylor [67,68] had already indicated that a dynamic method based on the dispersion of the component in a flowing stream of a second one, could be used. Indeed, the extension in the use of the quite successful in the case of measuring gaseous diffusion coefficients by chromatographic broadening techniques to liquid systems permitted the accumulation of precise and presumably accurate liquid diffusion coefficient data. However, the use of liquid mobile phase categorize it in liquid chromatography.

GC, being a dynamic technique, has been successfully used during the last three decades for the measurement of diffusion coefficients in a big number of gas–liquid systems, especially polymer–solvent ones.

From the 1980s, the chromatographic broadening technique has been "substituted" in the literature by inverses gas chromatography (IGC). In contrast with diffusion in the gas phase, where the point of interest is in the gas phase, in systems in which the diffusion coefficient in the liquid phase is measured, the liquid film deposited on the stationary phase is under investigation. The retention time of the solute and the shape of the elution peak reflect the strength and nature of the interactions that occur between the solute and the stationary phase. Such experiments referred in the literature to as IGC to differentiate them from the more common analytical applications of GC. The main application of IGC is physicochemical measurements [42,43] and the measurement of diffusion coefficients in liquids is one of those applications. GC-BT as well IGC use similar instrumentation and they are based on similar theoretical concepts. RF-GC, although being also an inverse gas chromatographic technique, is reviewed separately as in the case of gaseous diffusion coefficients.

3.1. Empirical equations

Diffusion in liquids has been studied for many years [67–105]. Available expressions for calculating diffusion coefficients in liquids, however, only partially have been successful. There is no one equation predicting diffusivities for all systems involving a liquid solvent.

In gas–liquid chromatography, we are usually interested in the diffusion of medium size solute molecules in the high molecular weight species of the stationary phase. In view of the fact that liquid molecules are more or less bound into place by rather strong intermolecular attractions, and must gain considerable thermal energy to break these bonds and achieve displacement, diffusional transport is logically an activation process with usual temperature exponential dependence:

$$D_{\mathrm{L}} = D_0 \exp\left(-\frac{E_{\mathrm{L}}}{RT}\right) \tag{32}$$

where E_{L} is the activation energy required for molecular displacement, R the ideal gas constant, T the absolute temperature and D_0 a term with only slight temperature variation. It has been observed that the activation energy E_{L} to be nearly equal for diffusional transport in liquids, D_{L}, and viscous shear of liquids, $1/\mu$. Since viscosity data are more prevalent (being easier to acquire) than diffusivities, we can obtain E_{L} by plotting $\log(1/\mu)$ versus $1/T$, from the slope $-E_{\mathrm{L}}/2.303R$ of the straight line obtained. According to the hole theories of liquids [69,70], the energy E_{L} is approximately equal to that needed to create the hole. However, Eyring [71] has also determined that the energy needed to create a hole in a liquid is one third of that needed to vaporize one of its molecules, assuming [70] that in GC, E_{L}, could be approximated by 0.35 times the heat of vaporization of solute from solvent, a parameter measured readily from GC data. The inadequacy of this assumption is shown by the fact that E_{L} may even exceed solute vaporization heats.

If it is desired to obtain numerical values for D_{L} itself, and not just of E_{L}, a large number of equations have been suggested with varying degrees of success [1,71–76]. Nearly all equations relate D_{L} to solvent viscosity μ_{B}. The first such equation was due to Einstein [76], which is known as the Stokes–Einstein equation:

$$D_{\mathrm{L}} = \frac{kT}{6\pi\mu_{\mathrm{B}}R_{\mathrm{A}}} \tag{33}$$

where R_{A} is the "radius" of the solute molecule and k the Boltzmann constant (subscript A applies to solute and B to solvent). Assuming a spherical molecule with molar volume V_{A}, this equation reduces to:

$$D_{\mathrm{L}} = \frac{10^{-7}T}{\mu_{\mathrm{B}}V_{\mathrm{A}}^{0.33}} \tag{34}$$

in which D_{L} ($\mathrm{cm^2\,s^{-1}}$) is inversely proportional to the cube root of solute molar volume V_{A} ($\mathrm{cm^3\,mol^{-1}}$) and solvent's viscosity μ_{B} (cp). The Stokes–Einstein equation was derived for large Brownian (colloid) particles, and is not applicable to solute molecules less than about 1000 in molecular mass.

Based on liquid structure and absolute rate theory approach, Eyring and co-workers [71] proposed an equation

designed for the diffusion of small molecules, particularly in cases of self diffusion. The equation is:

$$D_L = \frac{kT}{(\lambda_2\lambda_3/\lambda_1)\mu_B} \quad (35)$$

where λ's are molecular dimensions as defined in [71]. The term $\lambda_2\lambda_3/\lambda_1$ replaces $6\pi R_A$ of the Stokes–Einstein equation. It can be substituted by the ratio $(N_A/V_A)^{1/3}$ in which N_A is Avogadro's number. This term $(\lambda_2\lambda_3/\lambda_1)$ is smaller than $(6\pi R_A)$ by a factor of about 10 and therefore D_L is larger. The Eyring equation does not improve the accuracy of D_L calculations beyond the Stokes–Einstein equation, but it gives clear insight into the nature of liquid diffusion.

Othmer and Thakar [72] observed that $\log D_L$ is a linear function of $\log \mu_B$ and proposed the following empirical equation:

$$D_L = \frac{1.4 \times 10^{-4}}{V_A^{0.6}\mu_B\mu_{H_2O}^{(1.1\times\Delta H_{vapB}/\Delta H_{vapH_2O})}} \quad (36)$$

where μ_{H_2O} (cp) is the viscosity of water at the temperature of interest, ΔH_{vapB} is the enthalpy of vaporization of solvent and ΔH_{vapH_2O} the enthalpy of vaporization of water. At this point, it should be noted that the molar volumes V_A are determined as the summation of atomic volumes set forth by LeBass and as used previously by Gilliland and Arnold (see Section 2.1) in correlating coefficients in gases. The values of atomic volumes used are given in Table 15 [64,65,72]. Unfortunately, the Othmer and Thakar expression, cannot predict the temperature dependency of D_L and it is inaccurate for non-aqueous solvents.

The Wilke–Chang equation [73] is perhaps that with the best accuracy:

$$D_L = \frac{7.4 \times 10^{-8}(\psi_B M_B)^{0.5} T}{\mu_B V_A^{0.6}} \quad (37)$$

where M_B is the molecular weight of solvent, μ_B the viscosity of the solvent (cp), and V_A the molar volume of the solute ($cm^3\,mol^{-1}$) at the normal boiling point estimated by the values of Table 15. ψ_B is an association number of the solvent which is 2.6 for water, unity for non-polar solvent, 1.9 for methanol and 1.5 for ethanol. This equation is applicable to small and medium size molecules with an accuracy of about 10%. The main limitation is the association number which had to be calculated experimentally for polar systems. D_L is much more sensitive to the molecular size of the solute $(V_A^{0.6})$ than indicated by the Stokes–Einstein equation $(V_A^{-0.3})$.

Table 15
Atomic volumes, V_A ($cm^3\,mol^{-1}$) of various elements and compounds

Element	V_A	Element	V_A	Compound	V_A
C	14.8	N		H_2O	18.9
H	3.7	Double bonded	15.6	^2H_2O	22.0
Cl	24.6	Primary amines	10.5		
Br	27.0	Secondary amines	12.0		
I	37.0	O			
		Except as indicated	7.4		
		In methyl esters	9.1		
		In methyl ethers	9.9		
		In acids	12.0		
		Molecular oxygen	25.6		
		S	25.6		
		In benzene ring, deduct	15.0		
		In naphthalene ring, deduct	30.0		

Numerous other equations for D_L would require too much space and their presentation is beyond the scope of this work.

Summarizing the presentation of the empirical expressions related to the prediction of gas–liquid diffusion coefficients, D_L has a solvent, solute, temperature, as well as concentration dependence. The free-volume theory developed by Vrentas and Duda [77,78] is a good method for correlating and predicting diffusion in a polymer–solvent mixture. The free-volume theory reveals the effect of concentration and temperature of the solvent self-diffusion coefficient in a polymer solution.

3.2. The broadening techniques

3.2.1. Historical review

Although, neither partitioning nor adsorption is needed for diffusion determination, the chromatographic broadening technique was used by many workers for the measurement of liquid diffusivities.

The use of an open tube, introduced by Giddings and Seager [8] for the measurement of gaseous diffusivity seemed to be an obvious choice and in the case of liquid diffusivity. However, Giddings [79] suggested that such a column would have a microscopically rough surface, and that a glass bead column with liquid phase attached to dead contact points by capillary forces provided a better-defined liquid phase distribution. If it is assumed that a polymer coating on glass beads exists as a film of mean square thickness d_f^2, then the diffusion coefficient, D_L may be obtained by Gidding's form of the Van Deemter C term of Eq. (40).

Perrett and Purnell [80] presented a detailed study of the dependence of gas phase and liquid phase mass transfer contributions to theoretical plate height upon capacity ratio using packed columns in which liquid substrate was deposited on a solid support. However, they did not presented chromatographic experimental data concerning diffusivity in liquid phase.

The first utilization of the chromatographic broadening technique was done by Ouano [81] using a dynamic flowing system to measure diffusion coefficients. Pratt et al. [82] measured diffusion coefficients using GC-BT and computer manipulation of the recorded trace. The work of Balenovic et al. [27] in which they used GC-BT for obtaining diffusion coefficients in dense gases can also be cited.

Gray and Guillet in 1973 [83] based on Gidding's suggestion [79] measured the diffusion coefficient of hydrocarbons penetrants in a polyethylene stationary phase

prepared by deposition of polyethylene on glass beads (packed column broadening technique). In the next year, Grushka and Kikta [84] presented an extension of GC-BT method to liquid systems measuring diffusion coefficients of alkylbenzenes in chloroform from the width of the eluted peak. In their method a small amount of solute is injected into a flowing stream of a solvent. Consequently their column was empty. They showed that with a well-designed injection port, a small-volume detector cell, narrow tubing and low flow-rate, good diffusion data can be easily obtained. The dynamic character of the method permitted a rapid accumulation of data. Possible sources of error were also discussed. The precision of their system was estimated to be at about 1%. They stated that the precision and presumably the accuracy of the method will be substantially improved by computerization, in similarity to their work with gaseous systems [36]. Komiyana and Smith [85] and Jhaveri et al. [86] continued using the GC-BT for the measurement of diffusion coefficient in different liquid systems. Grushka and Kikta [87] extended their previous work [84] in the study of the dependence of the diffusion coefficients on molecular mass and on temperature. The diffusion coefficients of 12 phenones, ten with straight alkane side chains and two with branched chains, were measured at five temperatures ranging from 40 to 80 °C. They found that the diffusion coefficient decreases as the molecular weight increases. A linear relationship was found between the diffusion coefficient and the increment in the relative molecular weight increase. A linear correlation between the diffusion coefficient and the temperature was found and the contribution of each CH_2 group to the activation energy associated with liquid diffusion was determined to be 73 cal. They also determined the accuracy of the GC-BT method as used by them comparing their values with other experimental and theoretical ones from the Wilke–Chang [73] equation. Their data agreed very well with those determined by the Wilke–Chang equation, the larger deviation being 3% and fall between the two literature values used for the comparison.

From late 1970's IGC well established as an alternative technique for studying the interaction of polymers with volatile solutes [32,43,83]. IGC has been used primarily for the measurement of solution thermodynamics. In this way, parameters as the Henry's law constant, the activity coefficient and various solution interaction parameters were determined. In principle, IGC experiments can also be used to obtain information about the diffusion of the solute in the polymer phase. It has long been recognized that mass-transport limitations in the stationary phase result in a significant spreading and distortion of a chromatographic peak. A number of researchers have attempted to exploit this phenomenon as a means of measuring the diffusion coefficient of the solvent in the stationary phase [83,88–92]. In all of these studies, packed column inverse gas chromatography (PC-IGC) was used and diffusion coefficient estimates were extracted from the elution curve data using the Van Deemter equation. However, difficulties inherent in the use of a packed column made it nearly impossible to relate the measured elution curve to the diffusion coefficient. The major limitation was the irregular distribution of polymer within the column which prohibits the application of realistic models for stationary phase transport processes.

Pawlisch et al. [93,94] and Arnold and Laurence [95] developed and used effectively moment analysis models for the chromatographic process in capillary columns (capillary column IGC: CC-IGC) to measure diffusion coefficients in polymer–solvent systems. Pawlisch et al. [93] used capillary columns with highly uniform coatings of polymer and obtained data for the diffusion of toluene in polystyrene and ethylbenzene in polystyrene between 110 and 140 °C. Their data were consistent with existing vapor sorption measurements. However, information for the precision and accuracy of their method is not given.

Romdhane and Danner [96] presented a formulation of a new mathematical model to describe the elution process in packed columns, and to evaluate the moment analysis method for determining the partition and diffusion coefficients. They demonstrated the validity of their technique by measuring the diffusivity and solubility of toluene and benzene in polystyrene above the glass transition temperature of the polymer. Their diffusivity data were compared with previous results obtained by three other different techniques; capillary column IGC was one of them. Some systematic differences were found between their results and those reported by capillary column IGC. However, the precision and accuracy of their technique did not presented.

Jackson and Huglin [97] also used packed column IGC to measure diffusion coefficients of chlorobenzene in two types of cured (cross-linked) epoxy resin matrix at different temperatures. Their data analysis was done in terms of the Van Deemter equation.

Uriarte et al. [98] have also used packed column IGC and measured diffusion coefficients of *n*-octadecane in blends of phenoxy and poly(1,4-butylene adipate), at different temperatures above the thermal transitions of the stationary phases.

Danner et al. [99,100] extended the use of IGC on polymer–solvent systems to finite concentrations and to multicomponent systems. Packed column IGC and capillary column IGC, used for the measurement of diffusion coefficients of solvents in polymers at infinite solvent dilution, as well as the finite concentration IGC (FC-IGC), the multicomponent IGC (MIGC), and the fontal analysis by characteristic point IGC (FACP-IGC) are presented analytically in their paper [99].

Langenberg et al. [101] determined diffusion coefficients of SO_2 in cold sulfuric acid films by using capillary column IGC, on the basis of retention time and peak broadening.

In order to achieve a uniform distribution of polymer thickness, easy preparation of stationary phase and repeated use of the column, Huang et al. [102] designed rectangular thin-channel columns (RTCCs). By using RTCC inverse gas chromatography (RTCC-IGC) they determined partition and diffusion coefficients of small molecular weight solvents in

polymer membranes. The diffusion coefficient was related to the dimensionless second central moment of the elution curve of the solvent.

Some recent applications of GC for the measurement of diffusion coefficients in liquid systems can also be mentioned indicatively. Jiang et al. [103] determined infinite dilution coefficients of *n*-hexane, *n*-heptane and *n*-octane in polyisobutylene by packed column IGC and Balashova et al. [104] measured solubilities and diffusivities of solvent and non-solvents in polysulfone and polyetherimide by capillary column IGC.

3.2.2. Theoretical part

3.2.2.1. Packed column inverse gas chromatography. In this technique, a stationary phase prepared by deposition of the solvent on inert particles contained in a packed column is utilized. The interaction of the solute (mobile phase) with the solvent (stationary phase) is determined experimentally. As mentioned in the respective section for diffusion in gases, the Van Deemter equation describes the peak broadening. However, in a packed column the total broadening, measured again by the total variance, is obtained by adding the following two equations:

$$\sigma_1^2 = \frac{2D_{AB}L}{\bar{\upsilon}}\gamma \tag{38}$$

$$\sigma_2^2 = \frac{8}{\pi^2}\cdot\frac{d_f^2\bar{\upsilon}}{D_L}\cdot\frac{kL}{(1+k)^2} \tag{39}$$

where D_{AB} is the diffusion coefficient of the solute into the carrier gas due to longitudinal diffusion, k is the partition ratio of the solute in the packed column, d_f is the thickness of the liquid layer on the inert solid support, D_L the diffusion coefficient of the solute in the liquid layer of the stationary phase, t is the time elapsing from the pulse injection of solute and γ is the obstruction factor. The value of the partition ratio $k = (t_R - t_M)/t_M$ is calculated from the experimentally measured values of the retention time of the solute, t_R, and the retention time of the carrier gas to pass through the column, t_M.

By adding Eqs. (38) and (39) and dividing the resulting σ_{tot}^2 by L, the plate height of the column H is obtained as a function of $\bar{\upsilon}$, i.e. the Van Deemter equation:

$$H = A + \frac{2D_{AB}}{\bar{\upsilon}}\cdot\gamma + \frac{8}{\pi^2}\cdot\frac{d_f^2}{D_L}\cdot\frac{k}{(1+k)^2}\bar{\upsilon} \tag{40}$$

The term A is added to account for flow independent contributions to H. The linear portion of a graph of H versus $\bar{\upsilon}$ is used to calculate C in the Van Deemter equation. From the value of C, the ratio d_f^2/D_L is found accordingly to Eq. (40), but the problem is calculation of the thickness of the liquid layer, d_f. This is very difficult to be done accurately for packed columns, since the liquid phase is spread on porous supports in a complex way. However, a method to determine an average film thickness is available in literature [43]. With glass beads columns the film may be more uniform [79], permitting a more satisfactory evaluation of d_f. An alternative way is to calculate ratios of D_L, since the d_f values can be arranged to cancel. Or if D_L is known for one solute in one stationary phase, it is possible to estimate d_f for that stationary phase and hence D_L of any other solute in that stationary phase. The serious problem of non-uniformity with packed columns can be canceled by introducing the use of capillary columns. It should be noted that in the case of packed column IGC, D_L at infinite dilution are also obtained.

3.2.2.2. Capillary column inverse gas chromatography. In this technique, uniformly coated columns are made by filling a small capillary with a predetermined concentration of a degassed polymer solution. The liquid layer thickness can be specified precisely. An expression for the Laplace domain concentration profile at the exit of the column is obtained from the continuity equations for the solvent in the gas and polymer phases and the appropriate initial and boundary conditions. Accordingly to that expression the elution profile is a function of the three dimensionless parameters, α, β and Γ. α is inversely related to the partition coefficient, β is similarly related to the liquid diffusion coefficient, while Γ is proportional with the gas phase diffusion coefficient. A fast Fourier inverse transform is used to invert the solution of the CC-IGC model from the Laplace domain to the time domain. The first and the second moments of the elution profile are used to get initial estimates of K and D_L for the non-linear regression, which is carried out in order to minimize the error between the experimental data and model predictions. This analysis requires a linear sorption isotherm and a constant diffusion coefficient. The method for analyzing the response from a capillary column for an infinitely dilute input pulse has been presented analytically by Pawlisch et al. [93,94] and Arnold and Laurence [95], and Surana et al. [105].

3.2.2.3. Finite concentration inverse gas chromatography. In this IGC subtechnique, known as elution on a plateau, a uniform background concentration of the solvent is established in the carrier gas. D_L values at finite concentrations are obtained. A final non-dimensional equation in the Laplace domain, similar to that for the infinitely dilute region, is obtained taking into account the plateau concentration, $C_{plateau}$.

The elution profile is regressed in a similar way (cf. Section 3.2.2.2) to obtain the diffusion coefficient, D_L, and the partition coefficient, K. The only difference is that the measurements are at the finite concentration, $C_{plateau}$, in the gas phase. The method for analyzing the response at finite concentrations has been presented by Danner et al. [99].

3.2.2.4. Multicomponent inverse gas chromatography. IGC has also been used to measure the diffusion of an infinitely dilute component in a finite concentration of a second solvent in polymers. In this IGC subtechnique, once equilibrium has been established with a finite concentration

of one solvent, a pulse of another solvent is introduced. In recent works [99,100], the solvent pulse is infinitely dilute and the system is considered as a pseudo-binary system. Hence, the solvent concentration is taken as zero and its self-diffusion coefficient and partition coefficient in a matrix of the first solvent and the polymer are determined. The authors argue that an obvious extension of this method would be to establish finite concentrations of two solvents in the column and then introduce pulses of each of the solvents [99].

3.2.3. Experimental

In the experimental part, a brief presentation of the columns' preparation used by the two main IGC methods, namely the packed column and capillary column IGC, is done. More information about the theoretical and the experimental setup used by the various IGC subtechniques for the measurement of the liquid diffusivity in polymers is available in an excellent recent review by Danner et al. [99].

3.2.3.1. Packed column inverse gas chromatography. In packed column IGC, the preparation of the column is usually done by packing the column with a porous chromatographic material, running a solution of the solvent through it and removing the solvent by evaporating it with a stream of an inert gas. The presence of film irregularities due to the porous character of most chromatographic supports in packed columns is a problem, which affects the accuracy of the measured diffusion coefficients.

3.2.3.2. Capillary column inverse gas chromatography. An innovation in the use of IGC for the measurement of diffusion coefficients in liquids was the introduction of capillary columns, which solved the problem of the non-uniformity of the coating on the solid particles. A known concentration of a degassed solution is used to fill a capillary column, which is sealed at the one end and vacuum is applied to the other end. The evaporation of the solvent results in a deposition of uniform thin liquid layer on the capillary walls.

3.2.4. Results

A summary of literature data concerning diffusion coefficients of gases in liquids, determined by various IGC techniques, is given in Table 16.

3.3. The reversed-flow technique

3.3.1. Experimental

The experimental setup of the RF-GC method for measuring diffusion coefficients of gases in liquids, which has been described in detail elsewhere [106–109], is shown schematically in Fig. 12. A conventional gas chromatograph with a suitable detector system, contained in its oven two sections l' and l of a chromatographic column, empty of any material. The ends D_1 and D_2 of this column are connected to the carrier gas supply and the detector via a six-port valve.

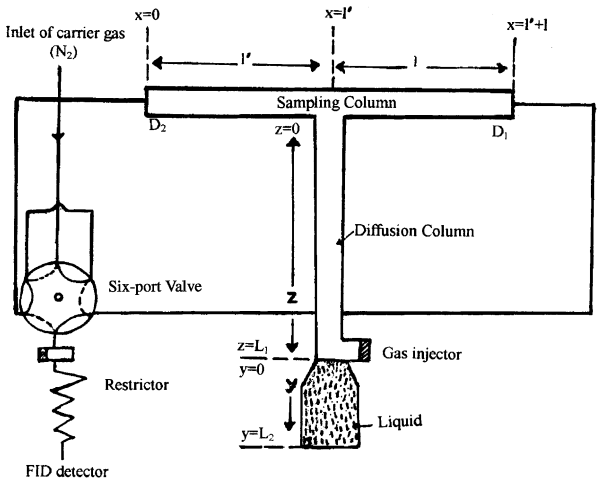

Fig. 12. Experimental setup of RF-GC technique for measuring diffusion coefficients of gases in liquids [108].

A diffusion column, consisted of the two sections z and y (cf. Fig. 12), are connected perpendicularly at its upper end to the middle of column $l' + l$. Section z with volume V_G, whilst section y with volume V'_G in which the liquid is contained. The carrier gas flows through the sampling column $l' + l$ either by entering at D_2 with the detector placed at D_1 or vice-versa. Through the injector, which was placed between the two regions z and y of the diffusion column, 1 cm^3 of the solute gas under study is introduced into the system, at various temperatures and at atmospheric pressure. The solute gas diffuses away along column L_1, while being also adsorbed by the liquid (e.g. water). When the gas reaches the junction $x = l'$, is carried by the carrier gas to the detector. After the injection of the solute gas and the wait for the monotonously rising concentration–time curve to appear in the detector signal, flow reversals for 6 s were effected by means of the six-port valve. When the gas is restored to its original direction, sample peaks, like those of Fig. 8 are recorded corresponding to various times from the beginning.

3.3.2. Theory

It has been shown [106–108] that each sample peak produced by a short flow reversal is symmetrical and its maximum height H from the ending baseline, when the lower part L_2 of the diffusion column is empty, is given by:

$$H^{1/M} = 2c(l', t) = \frac{6mD_{AB}}{\dot{V}L_1^2(1 + 3V'_G/V_G)} \cdot \exp\left(-\frac{3D_{AB}/L_1^2}{1 + 3V'_G/V_G}t\right) \quad (41)$$

where $c(l', t)$ is the solute concentration at $x = l'$ (cf. Fig. 12), the time t is measured from the moment of injection, m is the amount of solute injected, D_{AB} is the diffusion coefficient of solute into the carrier gas nitrogen, V_G and V'_G are the gaseous volumes in sections L_1 and L_2 of the diffusion column, respectively, and $\dot{V}$ is the volumetric flow-rate of the carrier gas in the sampling column. In that case the plot

Table 16
Diffusion coefficients of gases or vapors (A) in liquids (B), D_L ($cm^2\,s^{-1}$), measured by various inverse gas chromatographic techniques

Binary system		T (K)	D_L ($cm^2\,s^{-1}$)	Precision[a] (%)	Reference
A	B				
n-$C_{14}H_{30}$	Polyethylene	398.2	0.85×10^{-8}	–	[83]
		413.2	2.2×10^{-8}	–	[83]
		423.2	3.7×10^{-8}	–	[83]
		433.2	4.1×10^{-8}	–	[83]
		443.2	7.4×10^{-8}	–	[83]
n-$C_{10}H_{22}$	Polyethylene	303.2	0.35×10^{-8}	–	[83]
		323.2	1.03×10^{-8}	–	[83]
		333.2	1.00×10^{-8}	–	[83]
		338.2	1.28×10^{-8}	–	[83]
		353.2	1.34×10^{-8}	–	[83]
Benzene	Polyethylene	298.2	0.82×10^{-8}	–	[83]
Toluene	Polystyrene	403.0	2.79×10^{-9}	–	[96]
		403.0	1.95×10^{-9}	–	[96]
		413.0	8.61×10^{-9}	–	[96]
		413.0	8.41×10^{-9}	–	[96]
		423.0	28.8×10^{-9}	–	[96]
		433.0	83.3×10^{-9}	–	[96]
		433.0	78.2×10^{-9}	–	[96]
Benzene	Polystyrene	403.0	3.93×10^{-9}	–	[96]
		413.0	12.6×10^{-9}	–	[96]
		423.0	42.9×10^{-9}	–	[96]
		428.0	64.9×10^{-9}	–	[96]
		433.0	117.0×10^{-9}	–	[96]
Chlorobenzene	Amine epoxy resin	433.0	0.43×10^{-8}	9.3	[97]
		453.0	0.60×10^{-8}	25	[97]
		473.0	1.87×10^{-8}	17	[97]
		493.0	3.17×10^{-8}	28	[97]
	Anhydride epoxy resin	433.0	0.09×10^{-8}	14	[97]
		453.0	0.43×10^{-8}	16	[97]
		473.0	2.43×10^{-8}	25	[97]
		493.0	5.69×10^{-8}	20	[97]
n-Octadecane	Phenoxy (PH)	418.0	0.02724×10^{-8}	–	[98]
		423.0	0.04052×10^{-8}	–	[98]
		428.0	0.05398×10^{-8}	–	[98]
		433.0	0.11909×10^{-8}	–	[98]
n-Octadecane	Polybutylene adipate (PBA)	403.0	0.03679×10^{-8}	–	[98]
		408.0	0.04378×10^{-8}	–	[98]
		413.0	0.04938×10^{-8}	–	[98]
		418.0	0.05508×10^{-8}	–	[98]
n-Octadecane	PH/PBA (1:1)	403.0	0.00214×10^{-8}	–	[98]
		408.0	0.00246×10^{-8}	–	[98]
		413.0	0.00302×10^{-8}	–	[98]
		418.0	0.00372×10^{-8}	–	[98]
2-Ethylhexyl acrylate[b]	Polyacrylate	333.2	9.53×10^{-8}	–	[100]
		343.2	1.28×10^{-8}	–	[100]
		353.2	2.62×10^{-8}	–	[100]
		353.2	3.12×10^{-8}	–	[100]
		353.2	3.04×10^{-8}	–	[100]
		353.2	1.63×10^{-8}	–	[100]
		353.2	2.45×10^{-8}	–	[100]
		353.2	2.81×10^{-8}	–	[100]
		363.2	4.30×10^{-8}	–	[100]
2-Ethylhexyl acrylate[b]	Polyacrylate	373.2	5.38×10^{-8}	–	[100]
		373.2	8.26×10^{-8}	–	[100]
		373.2	10.7×10^{-8}	–	[100]
		373.2	1.46×10^{-8}	–	[100]
		373.2	3.86×10^{-8}	–	[100]

Table 16 (*Continued*)

Binary system		T (K)	D_L ($cm^2\ s^{-1}$)	Precision[a] (%)	Reference
A	B				
		373.2	6.86×10^{-8}	–	[100]
		373.2	2.62×10^{-8}	–	[100]
		373.2	6.48×10^{-8}	–	[100]
Ethyl acetate[b]	Polyacrylate	333.2	8.05×10^{-7}	–	[100]
		333.2	1.18×10^{-6}	–	[100]
		333.2	1.03×10^{-6}	–	[100]
		333.2	1.04×10^{-6}	–	[100]
		333.2	7.30×10^{-7}	–	[100]
		333.2	3.66×10^{-7}	–	[100]
		343.2	1.13×10^{-6}	–	[100]
		343.2	1.40×10^{-6}	–	[100]
		343.2	1.35×10^{-6}	–	[100]
		343.2	1.25×10^{-6}	–	[100]
		343.2	1.22×10^{-6}	–	[100]
		343.2	9.92×10^{-7}	–	[100]
		353.2	1.47×10^{-6}	–	[100]
		353.2	2.16×10^{-6}	–	[100]
		353.2	1.50×10^{-6}	–	[100]
		353.2	1.58×10^{-6}	–	[100]
		353.2	1.55×10^{-6}	–	[100]
		353.2	8.79×10^{-7}	–	[100]
		363.2	1.82×10^{-6}	–	[100]
		373.2	2.11×10^{-6}	–	[100]
		373.2	2.06×10^{-6}	–	[100]
		373.2	2.61×10^{-6}	–	[100]
		373.2	1.36×10^{-6}	–	[100]
		373.2	1.13×10^{-6}	–	[100]
		373.2	1.02×10^{-6}	–	[100]
C_2H_5OH	Cellulose diacetate	318.2	6.45×10^{-9}	–	[102]
		328.2	8.91×10^{-9}	–	[102]
		338.2	12.48×10^{-9}	–	[102]
	Sulfonated poly(ether ether ketone)	299.2	7.04×10^{-9}	–	[102]
		303.2	7.80×10^{-9}	–	[102]
		313.2	9.34×10^{-9}	–	[102]
1-Propanol[c]	Sulfonated poly(ether ether ketone)	299.2	7.12×10^{-9}	–	[102]
		303.2	7.70×10^{-9}	–	[102]
		299.2	6.96×10^{-9}	–	[102]
		303.2	7.47×10^{-9}	–	[102]
n-C_6H_{14}	Poly isobutylene	323.2	1.60×10^{-9}	–	[103]
		341.2	4.11×10^{-9}	–	[103]
		348.2	5.63×10^{-9}	–	[103]
		356.2	8.63×10^{-9}	–	[103]
		363.2	11.8×10^{-9}	–	[103]
n-C_7H_{16}	Poly isobutylene	323.2	0.48×10^{-9}	–	[103]
		341.2	1.57×10^{-9}	–	[103]
		348.2	2.03×10^{-9}	–	[103]
		363.2	4.40×10^{-9}	–	[103]
		373.2	6.83×10^{-9}	–	[103]
n-C_8H_{18}	Poly isobutylene	323.2	0.38×10^{-9}	–	[103]
		341.2	1.12×10^{-9}	–	[103]
		348.2	1.97×10^{-9}	–	[103]
		363.2	3.93×10^{-9}	–	[103]
		373.2	5.30×10^{-9}	–	[103]
Toluene	Polyisobutylene	323.2	0.35×10^{-9}	–	[103]
		341.2	1.59×10^{-9}	–	[103]
		348.2	1.92×10^{-9}	–	[103]
		356.2	2.35×10^{-9}	–	[103]
		363.2	3.03×10^{-9}	–	[103]
		373.2	4.24×10^{-9}	–	[103]

Table 16 (*Continued*)

Binary system		T (K)	D_L ($cm^2\ s^{-1}$)	Precision[a] (%)	Reference
A	B				
NMP	Polysulfone	473.2	7.40×10^{-9}	–	[104]
		493.2	3.33×10^{-8}	–	[104]
		523.2	2.30×10^{-7}	–	[104]
γ-Butyrolactone	Polysulfone	473.2	1.26×10^{-8}	–	[104]
		493.2	5.67×10^{-8}	–	[104]
		523.2	3.30×10^{-7}	–	[104]
Dimethyl sulfoxide (DMSO)	Polysulfone	473.2	1.20×10^{-8}	–	[104]
		493.2	6.30×10^{-8}	–	[104]
		523.2	3.20×10^{-7}	–	[104]
Acetic acid	Polysulfone	473.2	6.20×10^{-8}	–	[104]
		493.2	1.70×10^{-7}	–	[104]
		523.2	6.80×10^{-7}	–	[104]
Propionic acid	Polysulfone	473.2	2.45×10^{-8}	–	[104]
		493.2	9.40×10^{-8}	–	[104]
		523.2	4.75×10^{-7}	–	[104]
Water	Polysulfone	473.2	2.20×10^{-6}	–	[104]
		493.2	2.80×10^{-6}	–	[104]
		523.2	1.80×10^{-6}	–	[104]
THF	Polysulfone	473.2	1.60×10^{-8}	–	[104]
		493.2	6.90×10^{-8}	–	[104]
		523.2	3.60×10^{-7}	–	[104]
NMP	Polyetherimide	503.2	2.60×10^{-8}	–	[104]
		523.2	7.90×10^{-8}	–	[104]
		543.2	2.60×10^{-7}	–	[104]
γ-Butyrolactone	Polyetherimide	503.2	3.60×10^{-8}	–	[104]
		523.2	9.04×10^{-8}	–	[104]
		543.2	3.20×10^{-7}	–	[104]
DMSO	Polyetherimide	503.2	3.90×10^{-7}	–	[104]
		523.2	1.02×10^{-7}	–	[104]
		543.2	3.15×10^{-7}	–	[104]
Acetic acid	Polyetherimide	503.2	1.70×10^{-7}	–	[104]
		523.2	3.64×10^{-7}	–	[104]
		503.2	5.20×10^{-7}	–	[104]
Propionic acid	Polyetherimide	503.2	1.20×10^{-7}	–	[104]
		523.2	2.40×10^{-7}	–	[104]
		543.2	5.40×10^{-7}	–	[104]
Tetrahydrofuran	Polyetherimide	503.2	2.10×10^{-7}	–	[104]
		523.2	3.30×10^{-7}	–	[104]
		543.2	6.10×10^{-7}	–	[104]

[a] Precision as given by the authors. Otherwise precision has been defined as 100 × deviation/D_{AB}.
[b] The values referred to different mass fractions of component A.
[c] The values referred to different column lengths.

of $\ln H$ versus t (after the maximum) is linear during the whole experiment (cf. Fig. 13a).

When the lower part L_2 of the diffusion column is filled with a liquid (water), the diffusion band is distored in shape and/or in its slopes. The relevant equation describing this band depends on the rate by which the equilibrium state of the interaction between the solute gas and the liquid is established.

When the distribution equilibrium is rapidly established, the diffusion band (after the maximum) remains linear (cf. Fig. 13b), as in the situation when the vessel L_2 is empty, but its slope changes. In that case Eq. (41) can be written in the form [106]:

$$H^{1/M} = 2c(l', t) = \frac{6mD_{AB}}{\dot{V}L_1^2(1 + 3V'_G/V_G)} \cdot \exp\left(-\frac{3D_{AB}/L_1^2}{1 + 3(1 + k)V'_G/V_G}t\right) \quad (42)$$

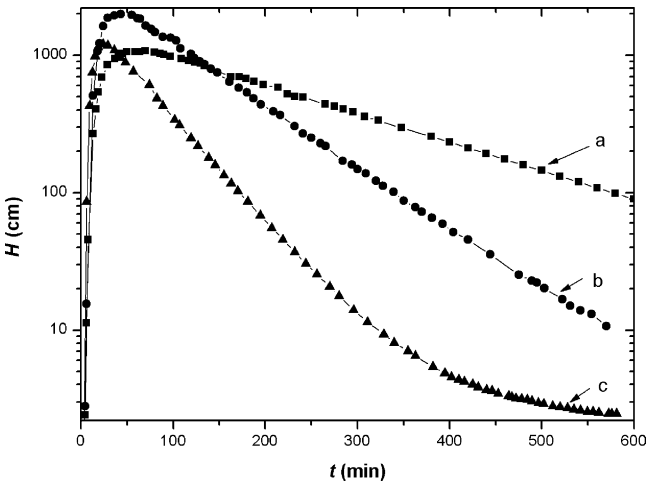

Fig. 13. Plot of H (in logarithmic scale) vs. t for vinylchloride and a vessel L_2 empty at 300.35 K (curve a) or filled with water at 300.35 K (curve b) and at 339.45 K (curve c) [108].

where k is the partition ratio of solute gas between the liquid and nitrogen.

In the case when the distribution equilibrium of the solute gas between the gas and the liquid phases is established slowly, there is a finite value for the overall mass transfer coefficient of solute between carrier gas and liquid and the diffusion band (after the maximum) is no longer linear, but distored, as shown in Fig. 13c. The relevant equation describing the descending part of this distortion, as a sum of two exponential function, is [106]:

$$H^{1/M} = 2c(l', t) = \frac{6mD_{AB}}{\dot{V}L_1^2(1+3V'_G/V_G)} \cdot \left[\left(1+\frac{Z}{Y}\right)\cdot \exp\left(-\frac{X+Y}{2}t\right) + \left(1-\frac{Z}{Y}\right)\cdot \exp\left(-\frac{X-Y}{2}t\right)\right] \quad (43)$$

where

$$X = \frac{3\beta + 72KaV_L/V_G + 25\pi^2(1+3V'_G/V_G)}{\pi^2(1+3V'_G/V_G)} \quad (44)$$

$$X^2 - Y^2 = \frac{300a(\beta + 16KaV_L/V_G)}{\pi^2(1+3V'_G/V_G)} \quad (45)$$

$$Z = X - 50a \quad (46)$$

$$a = \frac{\pi^2 D_L}{4L_2^2} \quad (47)$$

$$\beta = \frac{\pi^2 D_{AB}}{4L_1^2} \quad (48)$$

V_L is the volume of the liquid, D_L the diffusion coefficient of the solute gas in the liquid, and the partition coefficient K is the ratio of the liquid concentration of the gas at the interphase to that in the carrier gas.

There are two ways to calculate D_L from the diffusion band [106]:

First way: The sum of the two exponential coefficients of Eq. (43) gives the X value, while their difference gives the Y value. From the ratio of the two pre-exponential factors of the same equation:

$$\lambda = \frac{1 - Z/Y}{1 + Z/Y} \quad (49)$$

the value of Z can be found from the following relation:

$$Z = \frac{1-\lambda}{1+\lambda}Y \quad (50)$$

Combination of Eq. (50) with Eq. (46) gives the value of a, from which the D_L value can be computed via the Eq. (47).

Second way: The sum of the two exponential coefficients gives again the value of X, while their product $\prod$ equals $(X^2 - Y^2)/4$. If Eq. (44) is solved for $K\alpha V_L/V_G$ and the result is substituted into Eq. (45), one obtains a quadratic equation in a:

$$1250a^2 - 25\cdot\left[\frac{3\beta}{\pi^2(1+3V'_G/V_G)} + 2X\right]\cdot a + 3\pi = 0 \quad (51)$$

This on solution gives the value of $a = \pi^2 D_L/4L_2^2$ from which D_L is computed as L_2 is a known length.

3.3.3. Results and discussion

The method was applied for the determination of diffusion coefficients of various gases (ethene, propene, vinylchloride) into different liquids (water, heptane, hexadecane). The experimental results are compiled in Table 17, in which for comparison purposes literature data, as well as diffusion coefficients estimated from several semi-empirical methods have also been included [106–109]. The number of significant figures in the table is based on their standard errors as calculated from regression analysis. It is difficult to estimate the final error of the diffusion coefficients, since they come out as a result of a complex series of calculations as was described before.

The dispersion of the diffusion coefficient values around their mean value is not big, given that the experiments were conducted under widely varying conditions as regards the lengths L_1 and L_2 of the cell, and the volumes of the liquid V_L. It must be pointed out that there are not significant differences between the values found by using two completely different ways of calculation, which are based on different experimental data namely, the "first way" on the diffusion parameter β, and the "second way" on the pre-exponential factors of Eq. (43), as found from the intercepts of linear plots. This indicates the internal consistency of the theory.

The diffusion coefficients found by the RF-GC technique seem to be of the correct order of magnitude, and in some cases very close to those calculated using empirical equations [1,72,73,110–117], or reported in literature [117–121].

Table 17
Experimental diffusion coefficients (D_L^{exp}) of three gases in three liquids from RF-GC, as well as theoretical values (D_L^{theor}) estimated from various empirical equations, and literature ones (D_L^{lit}), at various temperatures and 1 atm

T (K)	System	No. of experiment	D_L^{exp} ($\times 10^5$ cm^2 s^{-1})		D_L^{theor} ($\times 10^5$ cm^2 s^{-1})	D_L^{lit} ($\times 10^5$ cm^2 s^{-1})
			First way	Second way		
294.2	Ethene–water	1	–	1.21	1.42 [73]	1.32 [118]
		2	–	1.40	1.34 [72]	1.41 [118]
					1.03 [111]	0.88 [117]
					1.45 [112,113]	1.36 [120,121]
					1.39 [115]	1.68 [119]
					2.16 [114]	
					2.17 [116]	
					0.93 [117]	
295.2	Ethene–heptane	1	4.36	3.04	5.33 [73]	
		2	3.41	1.65		
		3	3.08	1.30		
		4	3.60	2.12		
Mean value[a] ± S.E.			2.82 ± 0.37			
323.9	Propene–hexadecane	1	4.63	5.58	8.33 [73]	
		2	5.50	4.90		
		3	6.89	4.98		
Mean value[a] ± S.E.			5.41±0.33			
324.15	Vinylchloride–water	1	2.11	–	2.38 [73]	
329.05		1	1.75	–	2.62 [73]	
339.55		1	0.84	–	3.15 [73]	
345.45		1	0.66	–	3.49 [73]	

[a] These, together with their standard errors (S.E.), are calculated from the D_L values obtained in both ways.

They only disagreement of the experimental results with the theoretical predictions, is the decrease of the D_L^{exp} values with temperature for the diffusion of vinylchloride (VC) in water. It can be attributed to the fact that other than the liquid diffusion is the rate-determining step for the adsorption of VC by quiescent water. This should be either the dissolution process of VC into the water bulk, or the evaporation process of the liquid, which could hinder the liquid diffusion.

To overcome the big errors encountered in some cases for the determination of diffusion coefficients of gases in liquids by RF-GC, as well as to investigate the anomalous variation of D_L with temperature for the system VC–water, a new mathematical treatment was succeeded, which is presented in Ref. [122]. The final relation for the determination of D_L from the new version of RF-GC, by using the same experimental arrangement with that presented previously [106–109], is Eq. (22) of [122]:

$$D_L = \left(Y - \frac{2D_{AB}X}{L_1^2} - \frac{ZL_1^2}{2D_{AB}} + \frac{12D_{AB}^2}{L_1^4} \right) \frac{L_1^2 L_2^2}{24 D_{AB}} \quad (52)$$

where D_{AB} is the diffusion coefficient of VC into the carrier gas nitrogen, which either can be calculated from the empirical equations presented in Section 2.1, or can be experimentally determined by the RF-GG methods presented in Section 2.3.2, while the coefficients X, Y and Z, which are defined by the Eqs. (15)–(17) of [122], are functions of the exponential coefficients B_1, B_2 and B_3 of Eq. (18) in [122].

All calculations of D_L based on Eq. (52) can be carried out simultaneously by the GW-BASIC personal computer program, written for non-linear least-squares regression analysis [123–126] and based on the experimental pair values H, t, in cm and s, respectively.

It must be pointed out that except for the D_L values for the diffusion of VC in water, the partition coefficients of VC between the water (at the interface and the bulk) and the carrier gas nitrogen, the overall mass transfer coefficients of VC in the gas (nitrogen) and the liquid (water), the gas and liquid film transfer coefficients of VC, the gas and liquid phase resistances for the transfer of VC into the water, and finally the thickness of the stagnant film in the liquid phase, were also computed from the same personal computer program [122].

The diffusion coefficients of VC in water, determined by the new methodology of RF-GC, increase with temperature and are independent of the volume of water, as the theory predicts, but are dependent of the water-free surface area [122], probably due to the reason that the found D_L values do not express true but apparent diffusion coefficients, which maybe include partition and mass transfer coefficients.

Finally, the effect of surfactants on the diffusion coefficient of VC in water was investigated by RF-GC [127]. An interesting finding of this work was that by successive addition of surfactant in water, the critical micelle concentration of surfactant was obtained, after which follows a steady state for the diffusion of the VC gas into the water body,

which could be attributed to the transition from mono- to multi-layer state.

3.4. Sources of errors

The accuracy and reliability of IGC measurements is difficult to judge from the rather limited number of studies, primarily because of the dearth of reliable information with which to compare results. The IGC method has been subject to criticism that has doubt on the potential accuracy. The most serious concerns are summarized below:

(i) The Van Deemter analysis assumed a uniform distribution of the liquid phase. Therefore, the geometry of the stationary phase, should be well defined, so that a meaningful estimate of the thickness, d_f, of the liquid phase may be obtained. This demand rules out columns containing porous of a very complex structure solid supports. In general, in any real packed column the distribution is not uniform and will be difficult to characterize. The use of capillary columns can eliminate this concern.

(ii) A quantitative interpretation of the shape of the experimental Van Deemter plots requires firstly that the only significant source of peak broadening is due to slow equilibration through the stationary phase. Thus, instrumental dead volume and detector response time should be minimized, the isotherm relating vapor and stationary phase concentrations should be linear, and relatively thick stationary phase layers should be used.

(iii) The model also assumes that gas-phase axial dispersion is correctly described by an effective dispersion coefficient that is independent of the gas velocity. Because gas phase dispersive processes are responsible for a significant fraction of the peak broadening that occurs in a packed column, an accurate description of these processes is important. As a conclusion, capillary column IGC seems to be the best choise for reliable diffusivity data at infinite dilution.

3.5. Comparative study

(i) In comparison with conventional static methods used in the past, IGC offers several advantages. The main is the speed, as a single IGC experiment can be completed in minutes; a vapor sorption experiment requires hours or days to complete, while for a RF-GC experiment a duration of 6–10 h is necessary. The method of IGC is ideal for obtaining infinite dilution properties because very low solute concentrations can be measured with standard detector systems. In addition, changes in the solute and temperature can be readily made in a chromatographic experiment. These features enable determination of the interactions of a large number of solutes with a given liquid in a relatively short period of time.

(ii) The use of capillary columns has a number of significant advantages over packed columns in the IGC method. They have a simple geometry, with a thin and uniform coating, as well as there is less phase dispersion and there is no significant pressure drop. However, the mathematical analysis of the chromatographic data is more complex.

(iii) RF-GC belongs to IGC techniques. However, it is obvious from its experimental setup that it cannot categorized to anyone IGC subtechnique, as the liquid solvent is not deposited either on the surface of solid particles of a packing or on the surface of a capillary. RF-GC also estimates D_L values at conditions of infinite dilution, as the majority of IGC techniques.

(iv) The experimental setup used by RF-GC is much simpler than in the case of other IGC methods. The liquid solvent under study is easily put into a glass bottle at the closed end of the diffusion column. Therefore, the preparation of a RF-GC experiment is much simpler and less time consuming. By using RF-GC methodology, every gas–liquid pair can be practically studied.

(v) The uncertainty on the knowledge of the thickness of the liquid film, and the uniformity or non- of the liquid-layer deposited on solid particles or capillary column walls does not affect the D_L measurements by RF-GC. The volume and the mass of the liquid under study can easily and accurately measured in RF-GC experiments. Thus, fewer sources of errors affect D_L measurements.

(iv) The D_L values obtained by means of RF-GC are of the same order of magnitude and in some cases very close to those obtained by other techniques or calculated theoretically from empirical equations. The precision (∼13%), and the accuracy (8–47%) of the RF-GC method, as they are determined from the D_L values of Table 17, compared to those computed from the Wilke–Chang equation, are relatively satisfactory, considering the difficulties in obtaining experimental D_L values, and the large dispersion of the predicted, by different correlations, diffusion coefficients of ethene in water [119].

4. Surface diffusion

4.1. Introduction

One of the most fascinating phenomena associated with solid surfaces is the ability of the absorbed surface species to diffuse on the surface. This phenomenon is of great importance in catalysis, metallurgy, transport in porous media, and many other industrial and natural processes. According to the nature of the surface species, diffusion may be categorized into diffusion of physically adsorbed molecules, of chemisorbed species and self-diffusion. The latter refers to the diffusion of atoms, ions and clusters on the surfaces

of their own crystal lattices and has been studied more for metals.

On the other hand mass transfer kinetics in chromatographic columns contribute much to the performance achieved in both analytical and preparative applications. Retention data can be explained with a few simple thermodynamic models. By contrast, the mass transfer mechanisms of solutes in the stationary phase are complex, difficult to investigate and were paid relatively little attention although intraparticle mass transfer was and is actively studied in gas–solid and liquid–solid systems. According to Miyabe and Guiochon [128] most recent theoretical acquisitions in these areas remain ignored. Although it is now well known that the contribution of surface diffusion to intraparticle diffusion [129] is often important, this phenomenon and its contribution to mass transfer kinetics and column efficiency are still non-widely recognized in chromatography, although the significance of surface diffusion as one of the mass transfer mechanisms involved in this field was already described more than 30 years ago [1]. For instance, there are no plate height equations including a term accounting for the contribution of surface diffusion to column efficiency, even though some kind of lumped diffusivity experienced by sample molecules in the stationary phase film is taken into account on almost all plate height equations [1].

To date, most fundamental studies on surface diffusion have been made from the view-points of the dependence of D_s on temperature and the amount of adsorbed solute, in order to clarify the main characteristics of surface diffusion [129]. Surface diffusion is assumed to be an activated process, in similarity to liquid diffusion.

Surface diffusion has been observed and studied by many experimental techniques, dating back to the crystal growth experiments of Volmer and Estermann [130]. The most commonly used technique for measuring surface diffusion of adsorbed and chemisorbed species is the diffusion cell technique [131]. This technique has also been used for measuring binary or multicomponent diffusion. Many other techniques have also been employed to measure surface diffusion fluxes, including those on well-defined crystal surfaces. These techniques include the use of radioactive labeled adsorbates, infrared and electron spectroscopies, microscopies and low-energy electron diffraction. Furthermore, the invention of field emission microscopy and field ion microscopy enabled the observation of migration of individual adatoms or surface atoms and ions. Many other techniques including sintering, grain boundary grooves, and surface flattening have also been employed.

The majority of reported data for surface diffusion by chromatographic measurements are originated by groups using reversed phase liquid chromatography (RPLC). An excellent recent review on surface diffusion data by RPLC measured with various stationary phases, and mobile phases is available [132].

In principle, any technique that is capable of monitoring local adsorbate concentrations can be used to measure surface diffusion [129]. However, the only gas chromatographic method used for such measurement, in our knowledge, is RF-GC validating a recent mathematical analysis permitting the estimation of adsorption and desorption rate constants, local adsorbed concentrations, local isotherms, local monolayer capacities, energy distribution functions and consequently surface diffusion values in a single experiment [133,134].

4.2. Surface diffusion coefficients from reversed-flow gas chromatography

4.2.1. Experimental

Recently [133,134], the RF-GC technique has been successfully applied for the time-resolved determination of surface diffusion coefficients for physically adsorbed or chemisorbed species of CO, O_2 and CO_2 on heterogeneous surfaces of Pt/Rh catalysts supported on SiO_2. The experimental arrangement and procedure of RF-GC used have been described in detail many times [135–144] in studying the sorption processes of gases on solid surfaces, as well as the kinetics of surface-catalyzed reactions. All columns were accommodated inside the oven of a usual gas chromatograph (cf. Fig. 14) and were empty of any solid material, except for a short length L_2 (∼1.0 cm) at the closed end of the diffusion column, which contained the catalyst (0.1 g of 75% Pt + 25% Rh supported on SiO_2 (3%, w/w)). The separation column, which was filled with silica gel 80–100 mesh (∼7 g), was in another oven and its end was connected to a thermal conductivity detector. After conditioning of the catalyst, 1 cm^3 of the solute, under atmospheric pressure was rapidly introduced, with a gas-tight syringe, at the end of the diffusion column L. After a time of 5 min, a continuous concentration–time curve, owing to the adsorbate is established and recorded. During this period, flow reversals for 5 s were effected by means of the four-port valve, which gave rise to a series of sample peaks, like those of Fig. 5, their height H from the ending baseline

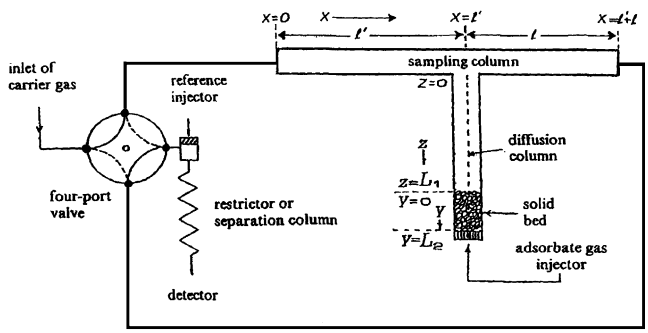

Fig. 14. Outline of the experimental arrangement for measuring surface diffusion coefficients by the reversed-flow gas chromatography method [133].

being a function of the time when the reversal was made [133,134]:

$$H^{1/M} = gc(l', t) = \sum_{i=1}^{4} A_i \exp(B_i t) \quad (53)$$

where the pre-exponential factors A_i and the corresponding coefficients of time B_i are easily and accurately determined from the pairs of H ant t by a personal computer program of non-linear least-squares regression [123–126].

4.2.2. Theoretical analysis

According to Jaroniec and Madey [145], the total diffusion coefficient, D_i, is divided into two parts: the term D_0 describing diffusion in the bulk phase, and the second term referring to the diffusion in the surface phase, D_s:

$$D_i = D_0 + D_s \frac{\partial\theta}{\partial p} \quad (54)$$

The pressure p reflects the concentration of the adsorbate in the bulk phase, and the adsorption isotherm θ reflects the concentration of the adsorbate in the surface phase. The surface diffusion coefficients D_s can be easily calculated from Eq. (54), since all other quantities are either known physical quantities, or can be obtained quite easily from the pairs H, t of the RF-GC experiments as follows: The total diffusion coefficient D_0 should be equal to $D_z\varepsilon_M^2$, i.e. to that of the adsorbate in the carrier gas in the absence of solid D_z, multiplied by the square of macro void fraction in the bed ε_M, according to the random-pore model [146]. This is required for boundary condition reasons at $z = L_1$ and $y = 0$. The D_0 term of Eq. (54) is equal to the experimental D_y (the total diffusion coefficient of the gas in the solid bed) calculated from the H, t pairs as described in [133].

There remains the partial derivative $\partial\theta/\partial p$ of Eq. (54) to be found. This is most easily done from Eq. (7) of [123].

$$\theta = 1 - \exp(-Kp) \quad (55)$$

where K is Langmuir's constant given by [123]

$$K = K^0 \exp\left(\frac{\varepsilon}{RT}\right) \quad (56)$$

K^0 being given by Eq. (9) of [123], and ε is the adsorption energy. Taking the partial derivative of θ with respect to p in Eq. (55) above, one simply finds:

$$\frac{\partial\theta}{\partial p} = K \exp(-Kp) = K(1-\theta) \quad (57)$$

Table 18
Time distribution of surface diffusion coefficient (D_s) for CO, O_2 and CO_2 gases adsorbed on 75% Pt + 25% Rh catalyst supported on SiO_2, at 593.8 K

CO		O_2		CO_2	
Time (min)	D_s ($cm^2\,s^{-1}$)	Time (min)	D_s ($cm^2\,s^{-1}$)	Time (min)	D_s ($cm^2\,s^{-1}$)
8	0.104	8	0.758	8	0.110
10	7.69×10^{-2}	10	0.294	10	7.03×10^{-2}
12	5.87×10^{-2}	12	0.162	12	5.42×10^{-2}
14	4.45×10^{-2}	14	0.94×10^{-2}	14	4.41×10^{-2}
16	3.26×10^{-2}	16	6.28×10^{-2}	16	3.57×10^{-2}
18	2.24×10^{-2}	18	3.86×10^{-2}	18	2.81×10^{-2}
20	1.38×10^{-2}	20	2.14×10^{-2}	20	2.12×10^{-2}
22	6.72×10^{-3}	22	8.89×10^{-3}	22	1.51×10^{-2}
24	1.10×10^{-3}	24	2.29×10^{-4}	24	9.76×10^{-3}
26	3.69×10^{-3}	26	7.72×10^{-3}	26	5.23×10^{-3}
28	9.04×10^{-3}	28	1.50×10^{-2}	28	1.51×10^{-3}
30	1.51×10^{-2}	30	2.23×10^{-2}	30	1.58×10^{-3}
32	2.19×10^{-2}	32	3.00×10^{-2}	32	4.93×10^{-3}
34	2.98×10^{-2}	34	3.85×10^{-2}	34	8.72×10^{-3}
36	3.90×10^{-2}	36	4.81×10^{-2}	36	1.30×10^{-2}
38	5.02×10^{-2}	38	5.99×10^{-2}	38	1.77×10^{-2}
42	8.32×10^{-2}	40	7.31×10^{-2}	40	2.31×10^{-2}
46	0.151	42	9.02×10^{-2}	42	2.90×10^{-2}
50	0.387	46	0.141	44	3.57×10^{-2}
56	0.605	50	0.241	46	4.33×10^{-2}
60	0.324	54	0.49	48	5.18×10^{-2}
64	0.256	58	1.85	50	6.14×10^{-2}
72	0.217	62	1.23	54	8.50×10^{-2}
80	0.211	66	0.789	58	0.116
88	0.216	72	0.616	62	0.158
96	0.227	80	0.563	66	0.213
104	0.243	88	0.544	70	0.289
112	0.262	106	0.561	76	0.456
120	0.285	114	0.578	82	0.724
–	–	122	0.597	86	0.987

and substituting it in Eq. (56) for K, there results:

$$\frac{\partial\theta}{\partial p} = K^0(1-\theta)\exp\left(\frac{\varepsilon}{RT}\right) \quad (58)$$

All three factors on the right-hand sides of Eqs. (57) and (58) above are easily calculated, namely K by Eq. (26) of [133], K^0 by Eq. (9) of [123], θ by Eq. (10) of [123], and ε or ε/RT by Eq. (56). Except for K^0, all other quantities are found from the values of A_1, A_2, A_3, A_4, B_1, B_2, B_3 and B_4 of Eq. (53), and the time parameter t. Thus, $\partial\theta/\partial p$ is found with a time-resolved procedure from the experimental chromatographic data H, t of the RF-GC method. Finally, the relation giving D_s is easily obtained from Eq. (54):

$$D_s = \frac{D_z\varepsilon_M^2 - D_y}{\partial\theta/\partial p} = \frac{D_z\varepsilon_M^2}{K^0(1-\theta)}\exp\left(-\frac{\varepsilon}{RT}\right) \quad (59)$$

4.2.3. Results and discussion

All calculations for the surface diffusion coefficients D_s from Eq. (59) can be carried out simultaneously by the GW-BASIC personal computer program listed in Appendix A of [133], by entering the H, t pairs in the DATA lines 3000–3040, together with the other experimentally determined quantities in the input lines 170–335. Except for the D_s values, adsorption energies, local adsorbed concentrations, local adsorption isotherms, adsorption and desorption rate constants, as well as total diffusion coefficients of the adsorbate gas in the solid bed, were also computed from the same personal computer program.

The surface diffusion coefficients of CO, O_2 and CO_2 in the 75% Pt + 25% Rh catalyst supported on SiO_2 are listed in Table 18, in a time-resolved procedure, showing clearly the dependence of D_s on time. The form of the above dependence does not coincide, however, exactly with that usually described in the past literature, although the orders of magnitude found are acceptable. For example, Slatek et al. [147] state that for chemisorption systems, the magnitude of reported D_s values range from 10^{-5} to 10^{-13} $cm^2\,s^{-1}$, usually considered below those characteristic of physical adsorption systems. The results presented in Table 18 range from 10^{-1} to 10^{-4} $cm^2\,s^{-1}$ at a relatively high temperature (ca. 600 K), except for the long time values being an order of magnitude higher.

The same methodology of RF-GC was also applied for the measurement of surface diffusion coefficients of CO on silica supported Rh catalyst under different conditions compatible with the operation of proton exchange membrane (PEM) fuel cells [134]. The calculated surface diffusion coefficients D_s cover a broad range of values (1×10^{-7} to 1×10^{0} $cm^2\,s^{-1}$) and show that chemisorption as well as physisorption of CO molecules occur. This is also a typical behavior of multilayer formation.

As a general conclusion one could say, that with a very simple modification of a commercial gas chromatograph, one can measure in a single experiment by RF-GC the surface diffusion coefficient in a time-resolved way, combined with a simultaneous measurement of the adsorption energy, the local adsorbed concentration, and the local adsorption isotherm, for gaseous adsorbates on heterogeneous solid surface. The results are in a relative agreement with those found by non-chromatographic techniques.

Acknowledgements

We thank Mrs. M. Barkoula for the technical preparation of the review.

References

[1] J.C. Giddings, Dynamics of Chromatography, Marcel Dekker, New York, 1965.
[2] J.O. Hirschfelder, C.F. Curtis, R.B. Bird, Molecular Theory of Gases and Liquids, Wiley, New York, 1954.
[3] R.B. Bird, W.E. Stewart, E.N. Lightfoot, Transport Phenomena, Wiley, New York, 1960.
[4] E.N. Fuller, P.D. Schettler, J.C. Giddings, Ind. Eng. Chem. 58 (1966) 19.
[5] E.N. Fuller, K. Ensley, J.C. Giddings, J. Phys. Chem. 73 (1969) 3679.
[6] T.-C. Huang, F.J.F. Young, C.-J. Huang, C.-H. Kuo, J. Chromatogr. 70 (1972) 13.
[7] T.R. Marrero, E.A. Mason, J. Phys. Chem. Ref. Data 1 (1972) 3.
[8] J.C. Giddings, S.L. Seager, J. Chem. Phys. 33 (1960) 1579.
[9] V.R. Maynard, E. Grushka, Adv. Chromatogr. 12 (1975) 99.
[10] J. Loschmidt, Sitzber Akad. Wiss. Wien 61 (1870) 367.
[11] J. Loschmidt, Sitzber Akad. Wiss. Wien 62 (1870) 468.
[12] E.P. Ney, F.C. Armstead, Phys. Rev. 71 (1947) 14.
[13] J. Stefan, Sitzber Akad. Wiss. Wien 68 (1873) 385.
[14] A.A. Westenberg, R.E. Walker, J. Chem. Phys. 26 (1957) 1753.
[15] J. Bohemen, J.H. Purnell, J. Chem. Soc. (1961) 360.
[16] P. Fejes, L. Czaran, Hung. Acta Chim. 29 (1961) 171.
[17] J.C. Giddings, S.L. Seager, Ind. Eng. Chem. Fundam. 1 (1962) 77.
[18] J.H. Knox, L. McLaren, Anal. Chem. 35 (1963) 449.
[19] S.L. Seager, L.R. Geertson, J.C. Giddings, J. Chem. Eng. Data 8 (1963) 168.
[20] J.H. Knox, L. McLaren, Anal. Chem. 36 (1964) 1477.
[21] E.N. Fuller, J.C. Giddings, J. Gas Chromatogr. 3 (1965) 222.
[22] G.T. Chang, Ph.D. Thesis, Rice University, TX, 1966.
[23] H.J. Arnikar, T.S. Rao, K.H. Karmarkar, J. Chromatogr. 26 (1967) 30.
[24] J.C. Giddings, K.L. Mallik, Ind. Eng. Chem. 59 (1967) 18.
[25] G.L. Hargrove, D.T. Sawyer, Anal. Chem. 39 (1967) 244.
[26] A.A. Zhukhovitskii, S.N. Kim, M.O. Burova, Zavod. Lab. 34 (1968) 144.
[27] Z. Balenovic, M.N. Myers, J.C. Giddings, J. Chem. Phys. 52 (1970) 915.
[28] S.P. Wasik, K.E. McCulloh, J. Res. Natl. Bur. Stand. US 73A (1969) 207.
[29] V.I. Lozgachev, O.A. Kancheeva, Russ. J. Phys. Chem. 46 (1972) 714.
[30] T.-C. Huang, S.-J. Sheng, F.J.F. Young, J. Chin. Chem. Soc. (Taipei) 15 (1968) 127.
[31] H.J. Arnikar, H.M. Ghule, Int. J. Electron. 26 (1969) 159.
[32] A.T.-C. Hu, R. Kobayashi, J. Chem. Eng. Data 15 (1970) 328.
[33] I. Nagata, T. Hasegawa, J. Chem. Eng. Jpn. 3 (1970) 143.
[34] J.C. Liner, S. Weissman, J. Chem. Phys. 56 (1972) 2288.
[35] E. Grushka, V. Maynard, J. Chem. Ed. 49 (1972) 565.
[36] E. Grushka, V. Maynard, J. Phys. Chem. 77 (1973) 1437.

[37] F. Young, S. Hawkes, F.T. Lindstrom, J. Am. Chem. Soc. 98 (1976) 5101.
[38] V.R. Choudhary, J. Chromatogr. 98 (1974) 491.
[39] S.M. Ashraf, R. Srivastava, A. Hussain, J. Chem. Eng. Data 31 (1986) 100.
[40] C.E. Cloete, T.W. Smuts, K.J. de Clerk, J. Chromatogr. 120 (1976) 17.
[41] V.R. Choudhary, M.G. Parande, J. Chromatogr. 132 (1977) 344.
[42] R.J. Laub, R.L. Pescok, Physico-Chemical Applications of Gas Chromatography, Wiley, New York, 1978.
[43] J.R. Conder, C.L. Young, Physico-Chemical Measurements by Gas Chromatography, Wiley, New York, 1979.
[44] B.K. Pathak, P.C. Singh, V.N. Singh, Can. J. Chem. Eng. 53 (1980) 38.
[45] B.K. Pathak, V.N. Singh, P.C. Singh, Can. J. Chem. Eng. 59 (1981) 363.
[46] C.S.G. Phillips, A.J. Hart-Davis, R.G.L. Saul, J. Wormald, J. Gas Chromatogr. 5 (1967) 424.
[47] N.A. Katsanos, G. Karaiskakis, D. Vattis, A. Lykourghiotis, Chromatographia 14 (1981) 695.
[48] R.C. Weast (Ed.), CRC Handbook of Chemistry and Physics, 58th ed., CRC Press, Cleveland, OH, 1977.
[49] N.A. Katsanos, I. Georgiadou, J. Chem. Soc., Chem. Commun. 242 (1980).
[50] N.A. Katsanos, Flow Perturbation Gas Chromatography, Marcel Dekker, New York, 1988.
[51] N.A. Katsanos, G. Karaiskakis, Adv. Chromatogr. 24 (1984) 125.
[52] N.A. Katsanos, F. Roubani-Kalantzopoulou, Adv. Chromatogr. 40 (2000) 231.
[53] N.A. Katsanos, R. Thede, F. Roubani-Kalantzopoulou, J. Chromatogr. A 795 (1998) 133.
[54] G. Karaiskakis, A. Niotis, N.A. Katsanos, J. Chromatogr. Sci. 22 (1984) 554.
[55] G. Karaiskakis, J. Chromatogr. Sci. 23 (1985) 360.
[56] N.A. Katsanos, G. Karaiskakis, J. Chromatogr. 237 (1982) 1.
[57] N.A. Katsanos, G. Karaiskakis, J. Chromatogr. 254 (1983) 15.
[58] N.A. Katsanos, V. Sotiropoulou, F. Roubani-Kalantzopoulou, H. Metaxa, Anal. Lab. 5 (1996) 13.
[59] K.R. Atta, D. Gavril, G. Karaiskakis, Instrum. Sci. Technol. 30 (2002) 67.
[60] K.R. Atta, D. Gavril, G. Karaiskakis, J. Chromatogr. Sci. 41 (2003) 123.
[61] St. Birbatakou, I. Pagopoulou, A. Kalantzopoulos, F. Roubani-Kalantzopoulou, J. Phys. Chim. 95 (1998) 2180.
[62] C.A. Boyd, N. Stein, V. Steingrimsson, W.F. Rumpel, J. Chem. Phys. 19 (1951) 548.
[63] D.H. Desty, C.J. Geach, A. Goldup, Gas Chromatography, Butterworths, London, 1960.
[64] J.H. Arnold, Ind. Eng. Chem. 22 (1930) 1091.
[65] E.R. Gilliland, Ind. Eng. Chem. 26 (1934) 681.
[66] G. Karaiskakis, N.A. Katsanos, A. Niotis, Chromatographia 17 (1983) 310.
[67] G. Taylor, Proc. Roy. Soc. Ser. A 219 (1953) 186.
[68] G. Taylor, Proc. Roy. Soc. Ser. A 225 (1954) 473.
[69] H. Eyring, J. Chem. Phys. 4 (1936) 283.
[70] H. Eyring, J. Chem. Phys. 5 (1937) 896.
[71] S. Glasstone, K.J. Laidler, H. Eyring, The Theory of Rate Processes, McGraw-Hill, New York, 1941.
[72] D. Othmer, M.S. Thakar, Ind. Eng. Chem. 45 (1953) 589.
[73] C. Wilke, P. Chang, AIChE J. 1 (1955) 264.
[74] R.C. Reid, T.K. Sherwood, Properties of Gases and Liquids, second ed., McGraw-Hill, New York, 1966.
[75] A. Akgerman, J. Gainer, J. Chem. Eng. Data 17 (1972) 372.
[76] A. Einstein, Z. Electrochem. 14 (1908) 1908.
[77] J.S. Vrentas, J.L. Duda, J. Polym. Sci. 15 (1977) 403.
[78] J.S. Vrentas, J.L. Duda, J. Polym. Sci. 15 (1977) 417.
[79] S.J. Hawkes, C.P. Russel, J.C. Giddings, Anal. Chem. 37 (1965) 1523.
[80] R.H. Perret, J.H. Purnell, Anal. Chem. 35 (1963) 430.
[81] A.C. Ouano, Ind. Eng. Chem. Fundam. 11 (1972) 268.
[82] K.C. Pratt, O.H. Slater, W.A. Wakeham, Chem. Eng. Sci. 28 (1973) 1901.
[83] D.G. Gray, J.E. Guillet, Macromolecules 6 (1973) 223.
[84] E. Grushka, E.J. Kikta, J. Phys. Chem. 78 (1974) 2297.
[85] H. Komiyama, J.M. Smith, J. Chem. Eng. Data 19 (1974) 384.
[86] P.F. Jhaveri, R.N. Trived, K. Vasudera, Chem. Abstr. 81 (1974) 68883.
[87] E. Grushka, E.J. Kikta, J. Am. Chem. Soc. 98 (1976) 643.
[88] W. Millen, S.J. Hawkes, J. Chromatogr. Sci. 15 (1977) 148.
[89] M. Gallin, M.C. Rupprecht, Polymer 19 (1978) 506.
[90] P.J.T. Tait, A.M. Abushihada, J. Chromatogr. Sci. 17 (1979) 219.
[91] G.A. Senich, Polym. Prep. 22 (1981) 343.
[92] D.S. Hu, C.D. Han, L.I. Stiel, J. Appl. Polym. Sci. 33 (1987) 551.
[93] G.A. Pawlisch, A. Macris, R.L. Laurence, Macromolecules 21 (1987) 1564.
[94] G.A. Pawlisch, J.R. Bric, R.L. Laurence, Macromolecules 20 (1988) 1685.
[95] D. Arnould, R.L. Laurence, in: D.R. Loyd, T.C. Ward, H.P. Shreiber (Eds.), Inverse Gas Chromatography (ACS Symposium Series, No. 391), American Chemical Society, Washington, DC, 1989, p. 87.
[96] I.H. Romdhane, R.P. Danner, AIChE J. 39 (1993) 625.
[97] P.L. Jackson, M.B. Huglin, Eur. Polym. J. 31 (1995) 63.
[98] C. Uriarte, J. Alfageme, A. Etxeberria, J.J. Iruin, Eur. Polym. J. 31 (1995) 609.
[99] R.P. Danner, F. Tihminlioglu, R.K. Surana, J.L. Duda, Fluid Phase Equilib. 148 (1998) 171.
[100] F. Tihminlioglu, R.P. Danner, J. Chromatogr. A 845 (1999) 93.
[101] S. Langenberg, V. Proksch, U. Schurath, Atmos. Environ. 32 (1998) 3129.
[102] R.Y.M. Huang, P. Shao, G. Nawawi, X. Feng, C.M. Burns, J. Membr. Sci. 188 (2001) 205.
[103] W.H. Jiang, H. Liu, H.J. Hu, S.J. Han, Eur. Polym. J 37 (2001) 1705.
[104] I.M. Balashova, R.P. Danner, P.S. Puri, J.L. Duda, Ind. Eng. Chem. Res. 40 (2001) 3058.
[105] R.K. Surana, R.P. Danner, F. Tihminlioglu, J.L. Duda, J. Polym. Sci. Part B 35 (1997) 1233.
[106] N.A. Katsanos, J. Kapolos, Anal. Chem. 61 (1989) 2231.
[107] D. Gavril, G. Karaiskakis, Instrum. Sci. Technol. 25 (1997) 217.
[108] D. Gavril, G. Karaiskakis, Chromatographia 47 (1998) 63.
[109] D. Gavril, K.A. Rashid, G. Karaiskakis, J. Chromatogr. A 919 (2001) 349.
[110] P.V. Danckwerts, Gas–Liquid Reactions, McGraw-Hill, New York, 1970, p. 15.
[111] A. Einstein, Ann. Physik. 17 (1905) 549.
[112] R.T. Ferrell, D.M. Himmelblau, AIChE J. 13 (1967) 702.
[113] R.T. Ferrell, D.M. Himmelblau, J. Chem. Eng. Data 12 (1967) 111.
[114] J. Houghton, J. Chem. Phys. 40 (1964) 1628.
[115] H.C. Longuet-Higgins, J.A. Pople, J. Chem. Phys. 25 (1956) 884.
[116] T.S. Ree, T. Ree, H. Eyring, J. Phys. Chem. 68 (1964) 3262.
[117] A.A. Unver, D.M. Himmelblau, J. Chem. Eng. Data 9 (1964) 428.
[118] A. Huq, T. Wood, J. Chem. Eng. Data 13 (1968) 256.
[119] M.H.I. Baird, J.F. Davidson, Chem. Eng. Sci. 16 (1962) 472.
[120] P.W. Dun, Ph.D. Thesis, University of Sydney, Australia, 1964.
[121] P.W. Dun, T. Wood, J. Appl. Chem. 16 (1966) 336.
[122] K.A. Rashid, D. Gavril, N.A. Katsanos, G. Karaiskakis, J. Chromatogr. A 934 (2001) 31.
[123] N.A. Katsanos, E. Arvanitopoulou, F. Roubani-Kalantzopoulou, A. Kalantzopoulos, J. Phys. Chem. B 103 (1999) 1152.
[124] Ch. Abatzoglou, E. Iliopoulou, N.A. Katsanos, F. Roubani-Kalantzopoulou, J. Chromatogr. A 775 (1997) 211.
[125] N.A. Katsanos, N. Rakintzis, F. Roubani-Kalantzopoulou, E. Arvanitopoulou, A. Kalantzopoulos, J. Chromatogr. A 845 (1999) 103.

[126] N.A. Katsanos, F. Roubani-Kalantzopoulou, J. Chromatogr. A 710 (1995) 191.
[127] K.A. Rashid, D. Gavril, V. Loukopoulos, G. Karaiskakis, J. Chromatogr. A 1023 (2004) 287.
[128] K. Miyabe, G. Guiochon, Anal. Chem. 72 (2000) 1475.
[129] A. Kapoor, R.T. Yang, C. Wong, Catal. Rev.-Sci. Eng. 31 (1989) 129.
[130] M. Volmer, J. Estermann, Z. Phys. 7 (1921) 13.
[131] E. Wicke, R. Kallenbach, Kolloid Z. 17 (1941) 135.
[132] K. Miyabe, G. Guiochon, Adv. Chromatogr. 40 (2000) 1.
[133] N.A.Katsanos.D. Gavril, G. Karaiskakis, J. Chromatogr. A 983 (2003) 177.
[134] V. Loukopoulos, D. Gavril, G. Karaiskakis, Instrum. Sci. Technol. 31 (2003) 165.
[135] D. Gavril, A. Koliadima, G. Karaiskakis, Langmuir 15 (1999) 3798.
[136] D. Gavril, G. Karaiskakis, J. Chromatogr. A 845 (1999) 67.
[137] D. Gavril, N.A. Katsanos, G. Karaiskakis, J. Chromatogr. A 852 (1999) 507.
[138] D. Gavril, A. Koliadima, G. Karaiskakis, Chromatographia 49 (1999) 285.
[139] N.A. Katsanos, E. Iliopoulou, V. Plagianakos, H. Mangou, J. Colloid Interf. Sci. 239 (2001) 10.
[140] D. Gavril, J. Liq. Chromatogr. Rel. Technol. 25 (2002) 2079.
[141] N.A. Katsanos, F. Roubani-Kalantzopoulou, E. Iliopoulou, I. Bassiotis, V. Siokos, M.N. Vrahatis, V.P. Plagianakos, Colloid Surf. A 201 (2002) 173.
[142] N.A. Katsanos, J. Chromatogr. A 969 (2002) 3.
[143] N. Bakaoukas, A. Koliadima, L. Farmakis, G. Karaiskakis, N.A. Katsanos, Chromatographia 57 (2003) 783.
[144] N.A. Katsanos, D. Gavril, J. Kapolos, G. Karaiskakis, J. Colloid. Interf. Sci., in press.
[145] M. Jaroniec, R. Madey, Physical Adsorption on Heterogeneous Solids, Elsevier, Amsterdam, 1988, p. 227.
[146] J.M. Smith, Chemical Engineering Kinetics, third ed., McGraw-Hill, New York, 1981, p. 467.
[147] K.J. Sladek, E.R. Gilliland, R.F. Baddour, Ind. Eng. Chem. Fundam. 13 (1974) 100.